Supporting Information

Carbazolylgold(III) Complexes with Thermally Activated Delayed Fluorescence Switched On by Ligand Manipulation as High Efficiency Organic Light-Emitting Devices with Small Efficiency Roll-Offs

Chun-Yin Wong,[a] Man-Chung Tang,[a] Lok-Kwan Li,[a] Ming-Yi Leung,[ab] Wai-Kit Tang,[a] Shiu-Lun Lai,[a] Wai-Lung Cheung,[a] Maggie Ng,[a] Mei-Yee Chan,[ab] Vivian Wing-Wah Yam*[ab]*

[a] Institute of Molecular Functional Materials and Department of Chemistry, The University of Hong Kong, Pokfulam Road, Hong Kong, P. R. China
Fax: +(852) 2857-1586; Tel: +(852) 2859-2153
E-mail: wwyam@hku.hk; chanmym@hku.hk

[b] Hong Kong Quantum AI Lab Limited
17 Science Park West Avenue
Pak Shek Kok, Hong Kong, P. R. China

Table of Contents

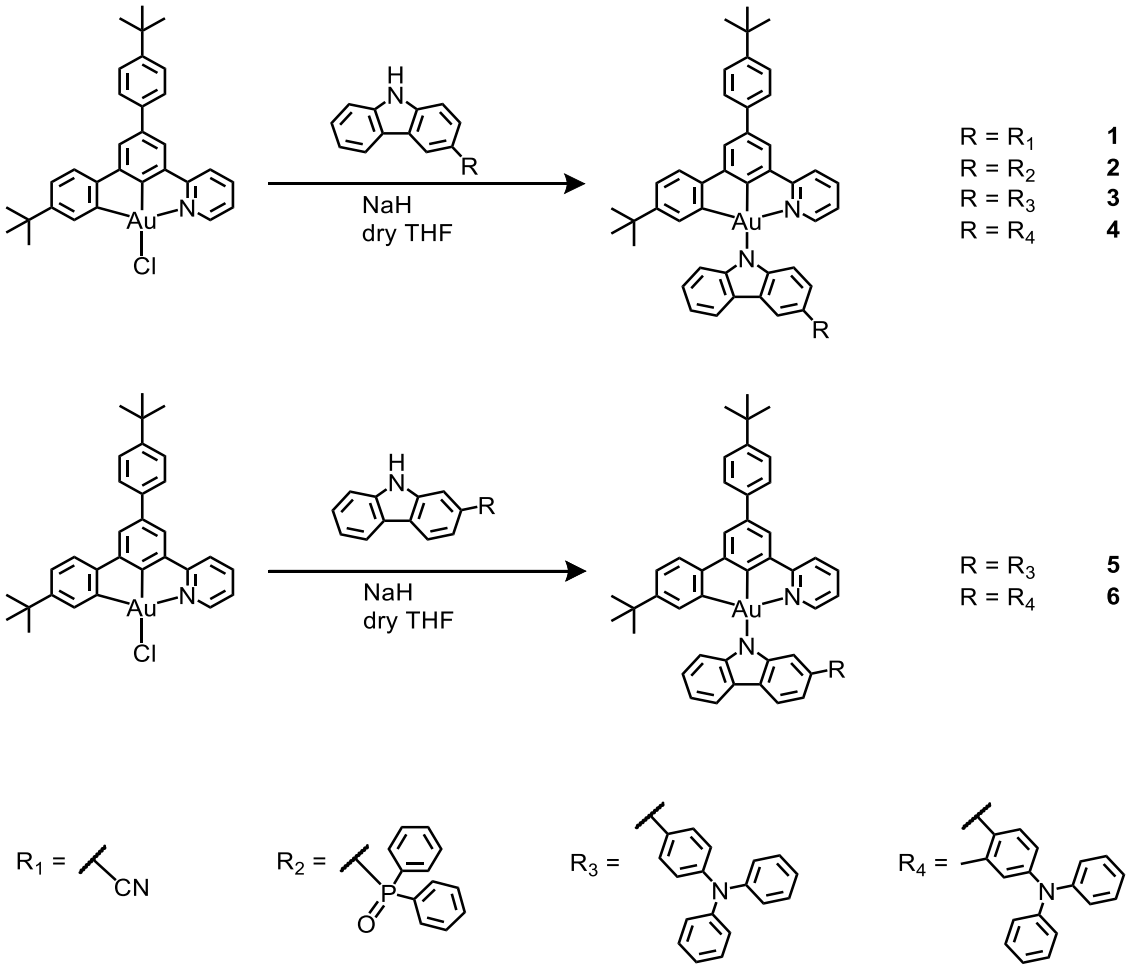

Scheme S1. Synthetic route for the carbazolylgold(III) complexes.

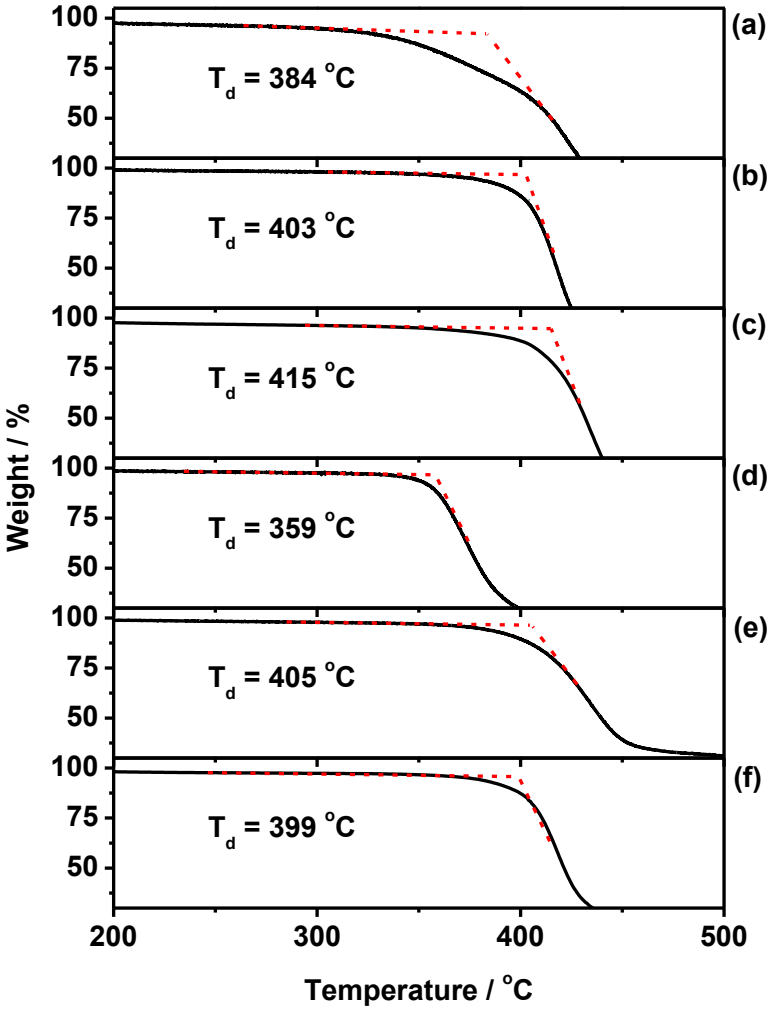

Figure S1. Thermogravimetric analysis (TGA) curves of (a) **1**, (b) **2**, (c) **3**, (d) **4**, (e) **5** and (f) **6**.

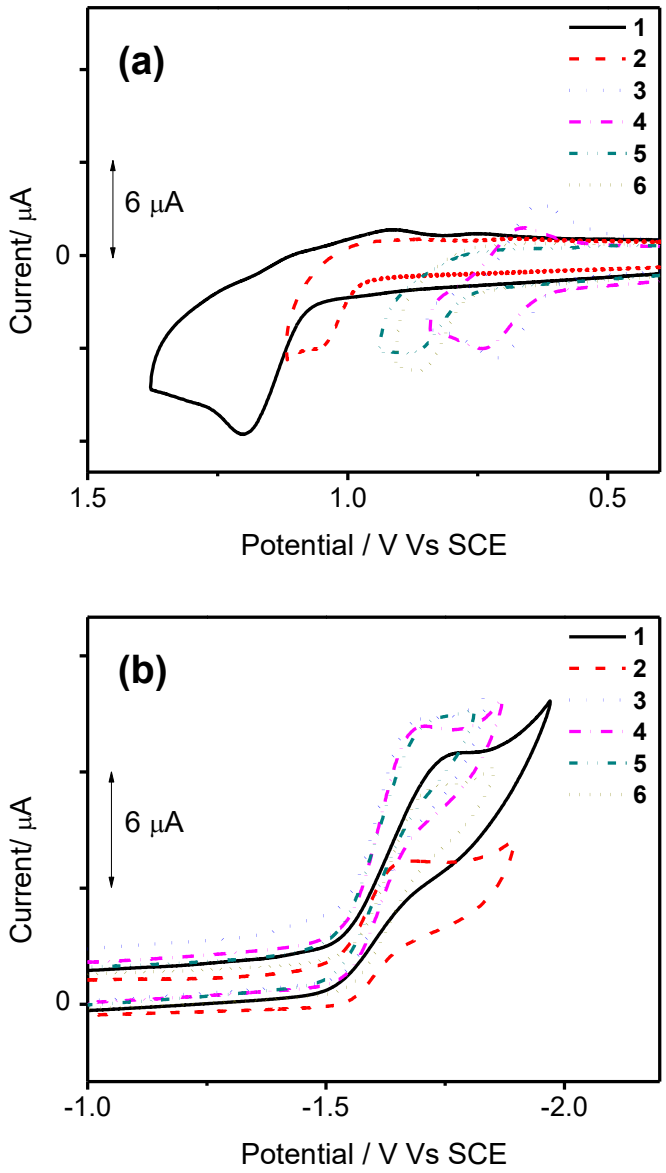

Figure S2. Cyclic voltammograms of (a) oxidation and (b) reduction scans of **1**–**6** in CH_2Cl_2 solution (0.1 M $^nBu_4NPF_6$).

Table S1. Electrochemical data of the gold(III) complexes.[a]

Complex	Oxidation $E_{1/2}$ / V *vs.* SCE[b] (ΔE_p / mV])[c] [E_{pa} / V *vs.* SCE][d]	Reduction [E_{pc} / V *vs.* SCE][e]	E_{HOMO} / eV[f]	E_{LUMO} / eV[g]
1	[+1.20]	[–1.73]	–5.54	–2.61
2	[+1.05]	[–1.65]	–5.39	–2.69
3	+0.67 (79), +0.95 (94)	[–1.68]	–5.01	–2.66
4	+0.70 (73), +0.93 (84)	[–1.69]	–5.04	–2.65
5	[+0.87], [+1.47]	[–1.71]	–5.21	–2.63
6	[+0.86], [+1.42]	[–1.70]	–5.20	–2.64

[a] In dichloromethane (CH_2Cl_2) solution with 0.1 M $^nBu_4NPF_6$ as supporting electrolyte at 298 K; working electrode, glassy carbon; scan rate = 100 mV s^{-1}.

[b] $E_{1/2} = (E_{pa} + E_{pc})/2$; E_{pa} and E_{pc} are the peak anodic and peak cathodic potentials, respectively.

[c] $\Delta E_p = (E_{pa} - E_{pc})$.

[d] E_{pa} refers to the anodic peak potential for the irreversible oxidation waves.

[e] E_{pc} refers to the cathodic peak potential for the irreversible reduction waves.

[f] E_{HOMO} levels were calculated from electrode potentials, i.e. $E_{HOMO} = -[E_{pa}$ (*vs.* Fc^+/Fc) + 4.80] eV or $E_{HOMO} = -[E_{1/2}{}^{ox}$ (*vs.* Fc^+ /Fc) + 4.80] eV. $E°(Fc^+/Fc) = +0.46$ V *vs.* SCE in CH_2Cl_2 (0.1 M $^nBu_4NPF_6$). From ref. 1.

[g] E_{LUMO} levels were calculated from electrode potentials, i.e. $E_{LUMO} = -[E_{pc}$ (*vs.* Fc^+/Fc) + 4.80] eV. $E°(Fc^+/Fc) = +0.46$ V *vs.* SCE in CH_2Cl_2 (0.1 M $^nBu_4NPF_6$). From ref. 1.

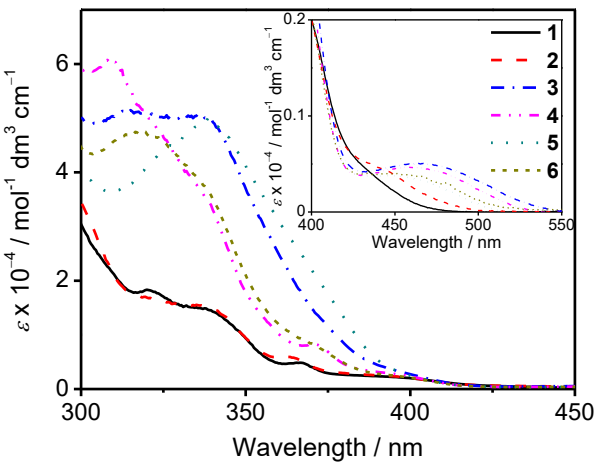

Figure S3. UV-Vis absorption spectra of **1**–**6** in toluene at 298 K.

Table S2. Electronic absorption data of the gold(III) complexes in toluene at 298 K.

Complex	Absorption λ_{max} / nm (ε_{max} / mol^{-1} dm^3 cm^{-1})
1	320 (18160), 340 (14260), 366 (4740), 401 (2075)
2	341 (14860), 365 (5620), 402 (1840), 445 (430)
3	313 (51285), 337 (50330), 400 (2625), 465 (505)
4	309 (60595), 337 (35350), 371 (8055), 396 (2670), 462 (460)
5	323 (42910), 338 (49175), 397 (2880), 454 (360)
6	317 (46965), 338 (37110), 371 (8280), 398 (2355), 454 (400)

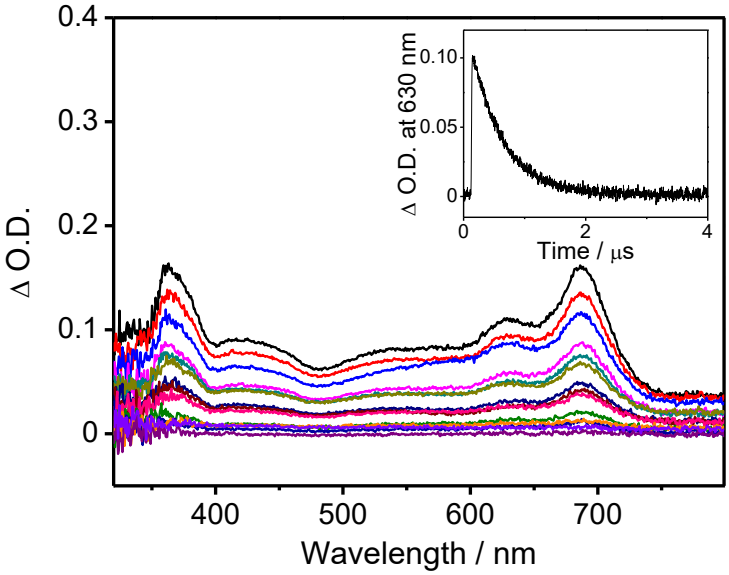

Figure S4. Transient absorption spectra of **6** in degassed toluene at 298 K at decay times of 0−2 μs and the decay trace monitored at 630 nm in the inset.

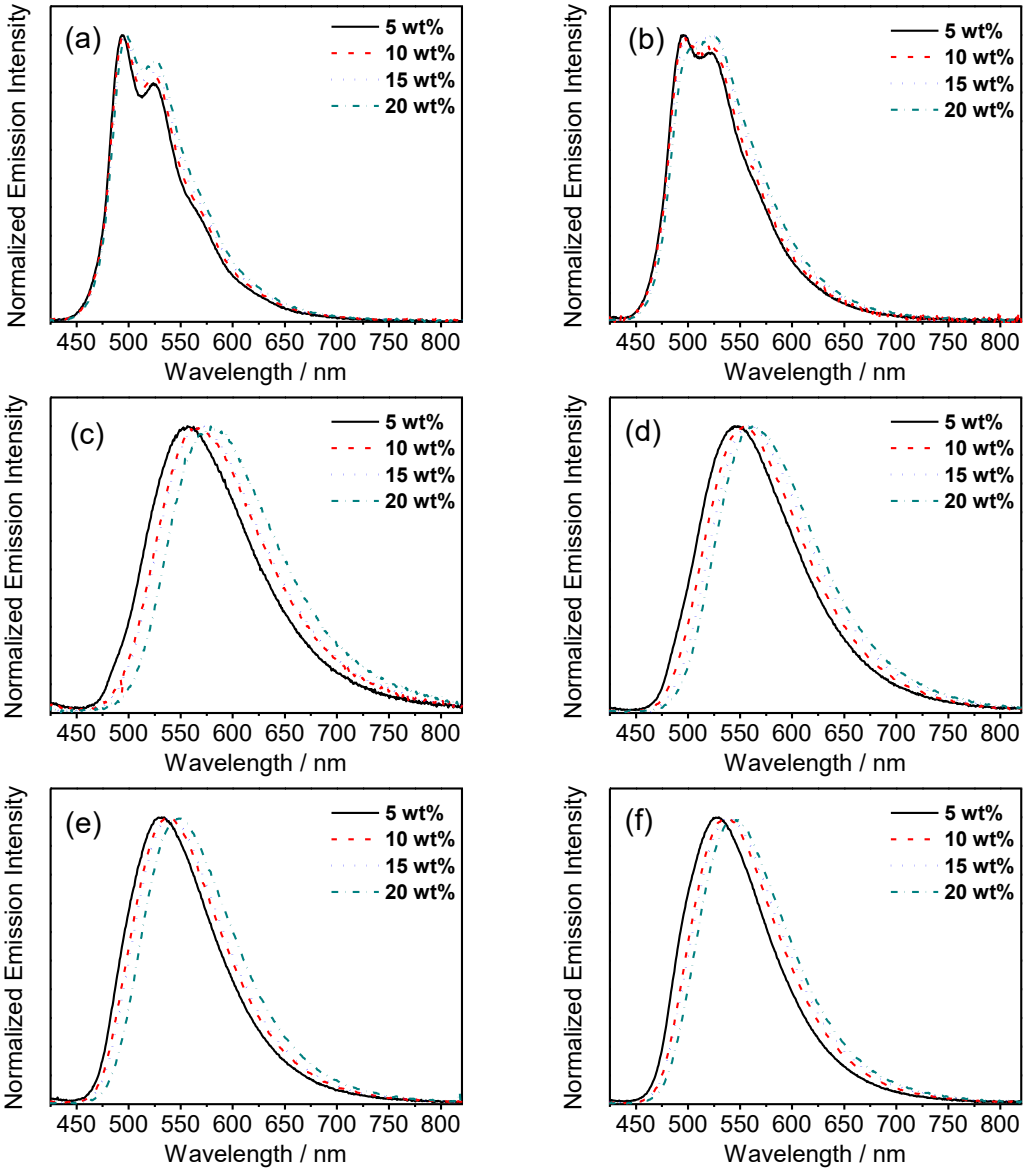

Figure S5. Normalized PL spectra of thin films of (a) **1**, (b) **2**, (c) **3**, (d) **4**, (e) **5** and (f) **6** doped into MCP at 298 K.

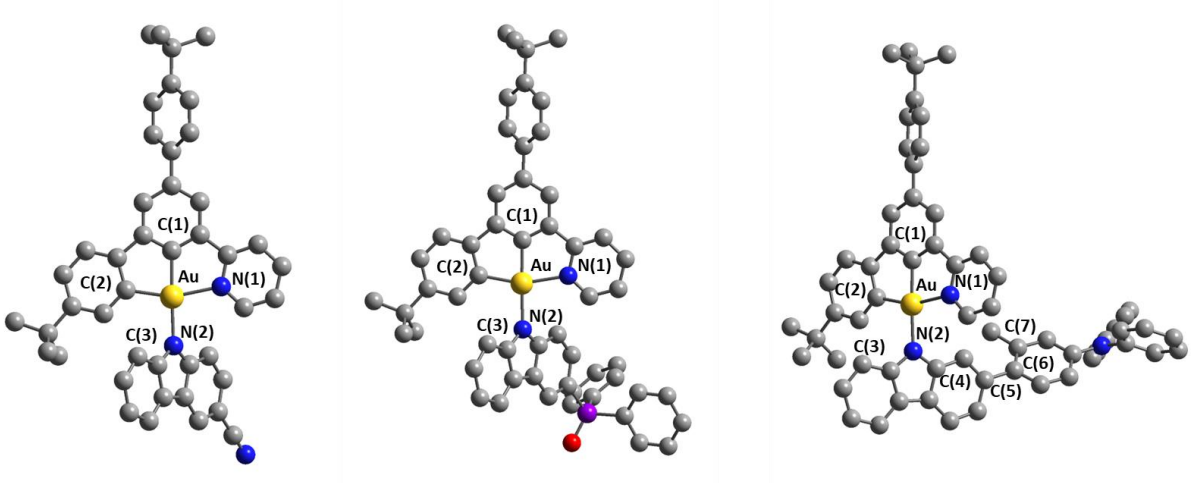

Au–C(1)	1.962
Au–C(2)	2.017
Au–N(1)	2.165
Au–N(2)	2.079
N(1)–Au–C(1)	79.3
C(1)–Au–C(2)	81.1
C(2)–Au–N(2)–C(3)	60.7

1

Au–C(1)	1.962
Au–C(2)	1.962
Au–N(1)	2.166
Au–N(2)	2.075
N(1)–Au–C(1)	79.2
C(1)–Au–C(2)	81.1
C(2)–Au–N(2)–C(3)	61.0

2

Au–C(1)	1.963
Au–C(2)	2.016
Au–N(1)	2.166
Au–N(2)	2.073
N(1)–Au–C(1)	79.2
C(1)–Au–C(2)	81.1
C(2)–Au–N(2)–C(3)	57.4
C(4)–C(5)–C(6)–C(7)	50.7

6

Figure S6. Selected structural parameters of the ground-state geometries of **1**, **2** and **6** optimized at the PBE0 level of theory. All hydrogen atoms are omitted for clarity. The bond lengths and bond angles are in Angstrom and degrees, respectively.

Table S3. The first fifteen singlet (S_n) excited states computed by TDDFT/CPCM (toluene) at the optimized ground-state geometries.

Complex	S_n	Excitation[a] (Coefficient)[b]	Vertical excitation wavelength / nm	f [c]
1	S_1	H→L (0.70)	463	0.007
	S_2	H−2→L (0.69)	381	0.073
	S_3	H−1→L (0.70)	373	0.000
	S_4	H→L+1 (0.70)	372	0.006
	S_5	H−3→L (0.67)	332	0.077
	S_6	H→L+2 (0.68)	330	0.032
	S_7	H→L+3 (0.64)	328	0.025
	S_8	H−2→L+1 (0.58)	321	0.068
		H−2→L+1 (0.30)		
	S_9	H→L+4 (0.61)	320	0.092
	S_{10}	H−1→L+1 (0.70)	313	0.001
		H−1→L+4 (0.33)		
	S_{11}	H→L+6 (0.51)	295	0.087
		H→L+7 (0.51)		
	S_{12}	H−4→L (−0.33)	294	0.040
	S_{13}	H−2→L+3 (0.55)	292	0.018
	S_{14}	H−3→L+1 (0.41)	291	0.121
	S_{15}	H−2→L+2 (0.57)	283	0.012
2	S_1	H→L (0.70)	485	0.007
	S_2	H−1→L (0.70)	389	0.000
	S_3	H→L+1 (0.70)	386	0.006
	S_4	H−2→L (0.69)	381	0.071
	S_5	H→L+2 (0.70)	340	0.035
	S_6	H→L+3 (0.66)	335	0.027
	S_7	H−3→L (0.66)	331	0.070
	S_8	H−1→L+1 (0.70)	324	0.002
	S_9	H−2→L+1 (0.65)	321	0.097
	S_{10}	H→L+4 (0.59)	320	0.058
	S_{11}	H−4→L (0.64)	296	0.038
	S_{12}	H−3→L+1 (0.36)	292	0.076
		H→L+5 (−0.35)		
	S_{13}	H→L+5 (0.39)	292	0.020
		H→L+6 (0.32)		
	S_{14}	H−1→L+2 (0.46)	292	0.022
		H→L+7 (0.32)		
	S_{15}	H−2→L+3 (0.66)	290	0.004
6	S_1	H−1→L (0.65)	511	0.006

S_2	H→L (0.65)	479	0.000
S_3	H−1→L+1 (0.65)	403	0.004
S_4	H−2→L (0.69)	397	0.001
S_5	H→L+1 (0.64)	386	0.009
S_6	H−3→L (0.69)	380	0.071
S_7	H−1→L+2 (0.64)	353	0.048
S_8	H−1→L+4 (0.64)	347	0.040
S_9	H→L+2 (0.54)	338	0.327
	H→L+3 (−0.33)		
S_{10}	H−1→L+3 (0.47)	335	0.172
	H→L+3 (0.38)		
S_{11}	H−1→L+3 (0.46)	332	0.431
	H→L+3 (−0.40)		
S_{12}	H−2→L+1 (0.68)	331	0.005
S_{13}	H−4→L (0.68)	330	0.122
S_{14}	H−3→L+1 (0.67)	321	0.123
S_{15}	H→L+6 (0.54)	315	0.018
	H→L+4 (−0.38)		

[a] The orbitals involved in the excitation (H = HOMO and L = LUMO).

[b] The coefficients in the configuration interaction (CI) expansion that are less than 0.3 are not listed.

[c] Oscillator strengths.

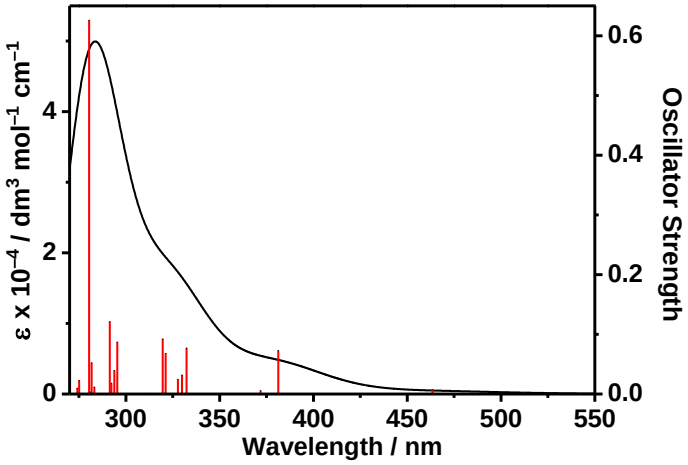

Figure S7. Simulated absorption spectrum of **1**. The heights of the vertical straight lines are the calculated oscillator strengths of the corresponding vertical transitions.

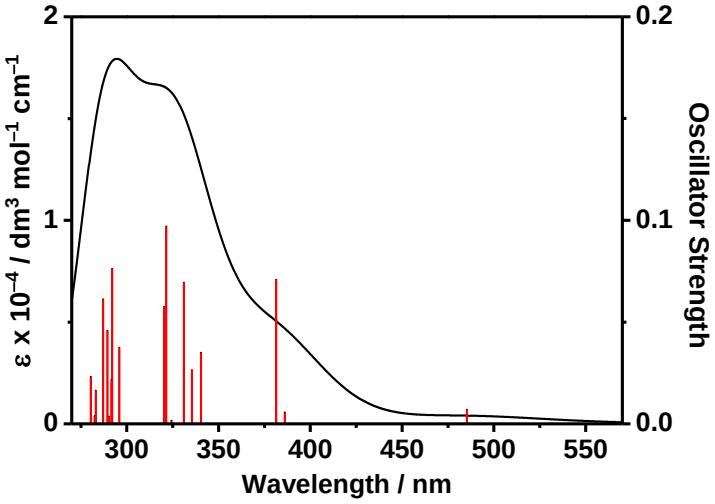

Figure S8. Simulated absorption spectrum of **2**. The heights of the vertical straight lines are the calculated oscillator strengths of the corresponding vertical transitions.

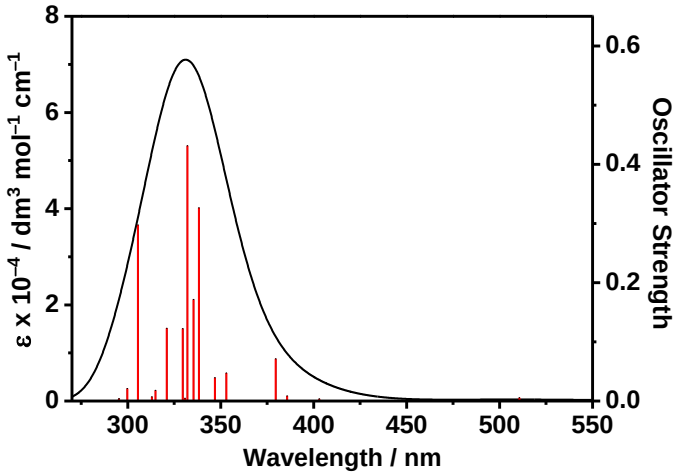

Figure S9. Simulated absorption spectrum of **6**. The heights of the vertical straight lines are the calculated oscillator strengths of the corresponding vertical transitions.

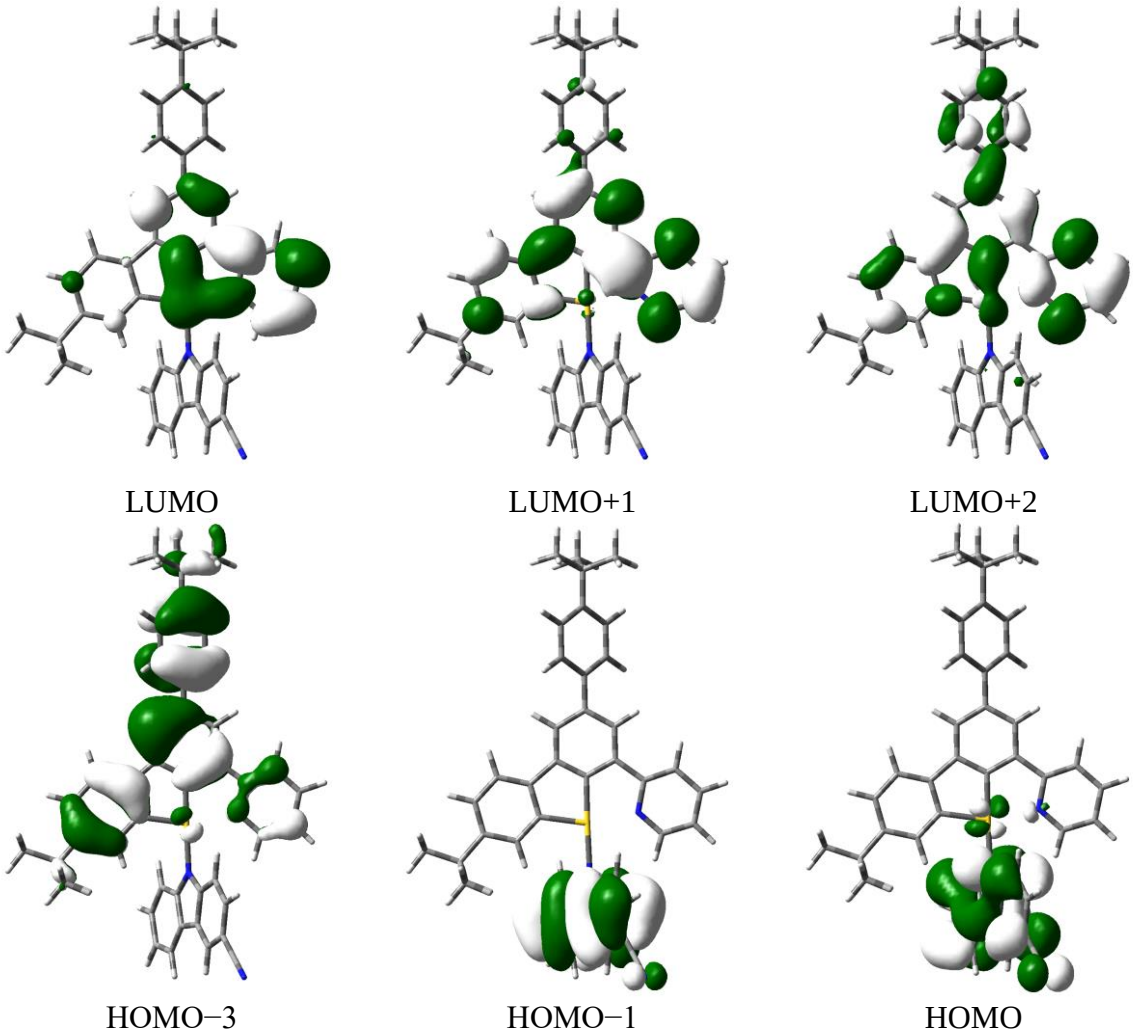

Figure S10. Spatial plots (isovalue = 0.03) of selected molecular orbitals of **1** at the optimized ground-state geometry.

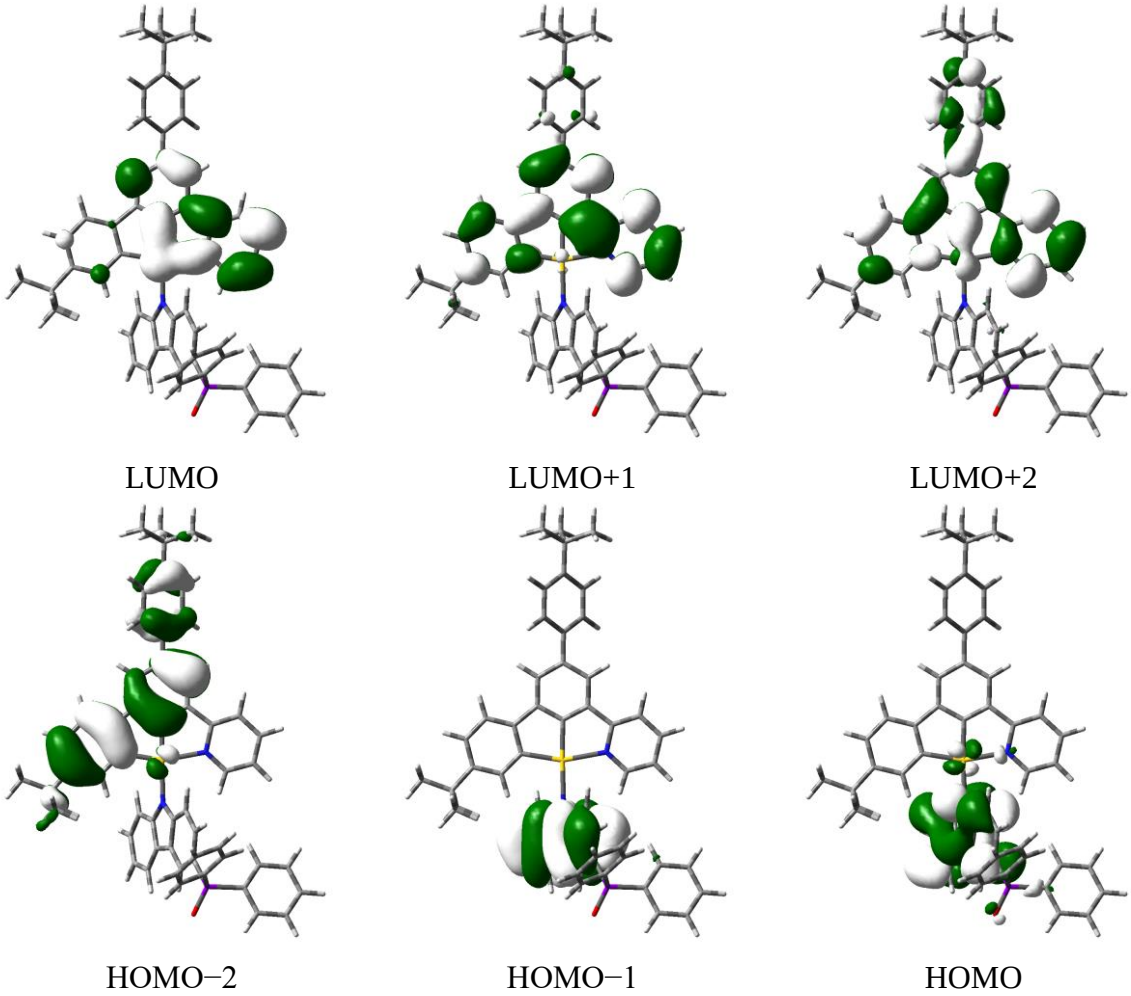

Figure S11. Spatial plots (isovalue = 0.03) of selected molecular orbitals of **2** at the optimized ground-state geometry.

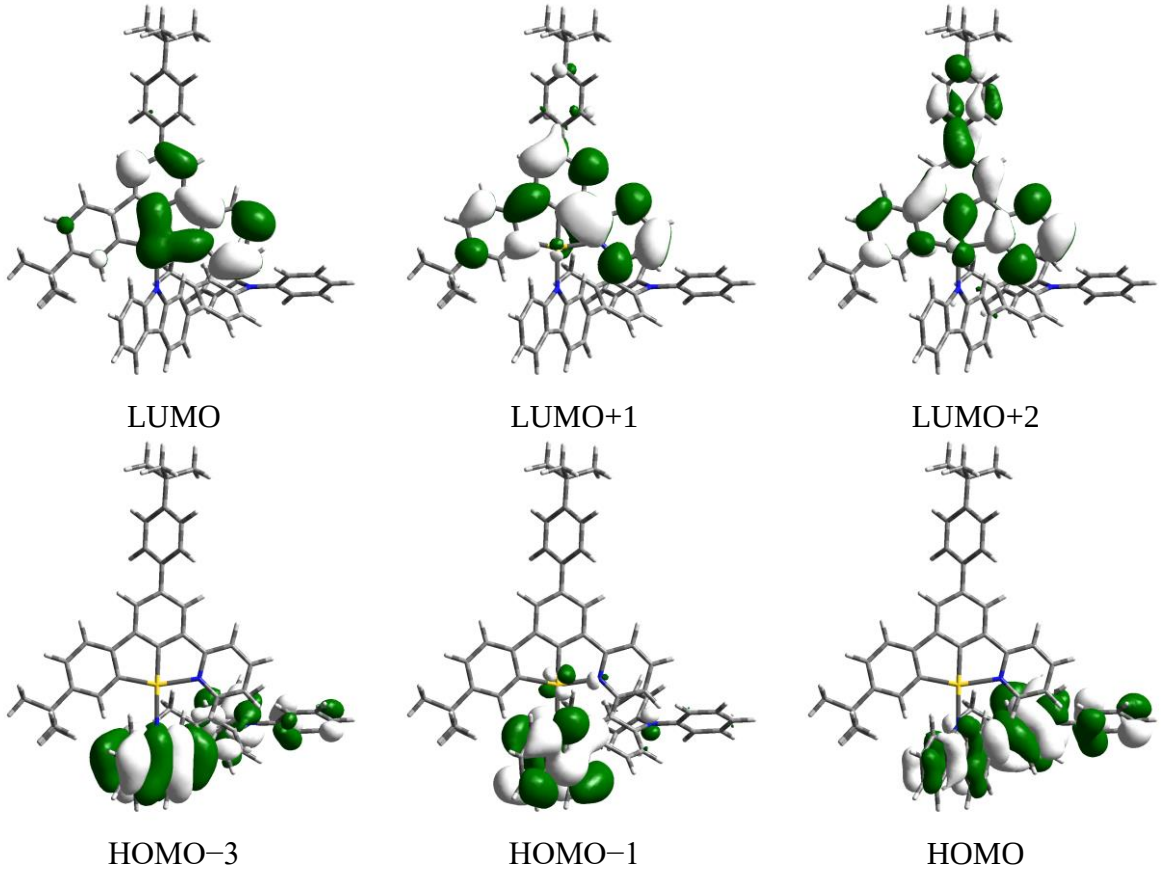

Figure S12. Spatial plots (isovalue = 0.03) of selected molecular orbitals of **6** at the optimized ground-state geometry.

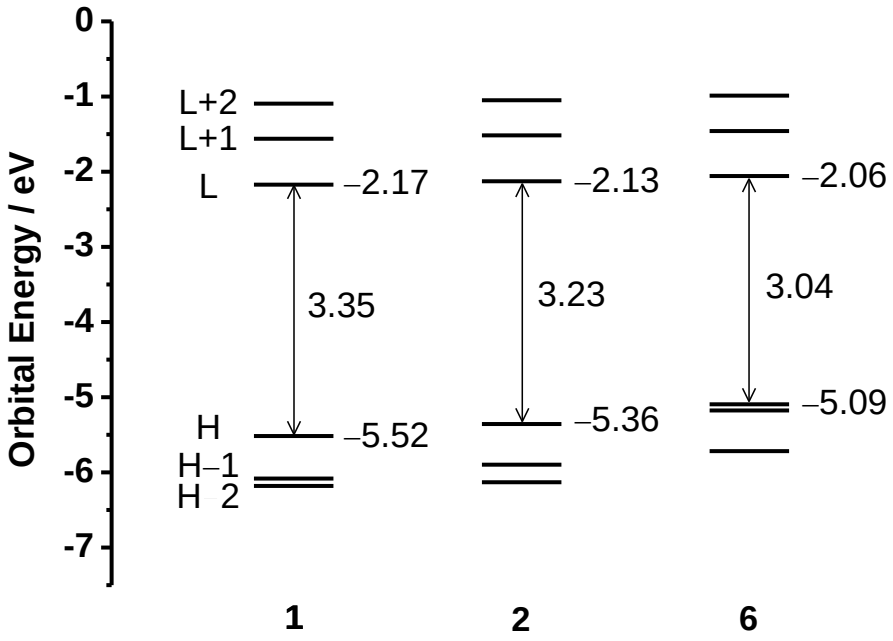

Figure S13. Orbital energy diagram of **1**, **2** and **6**.

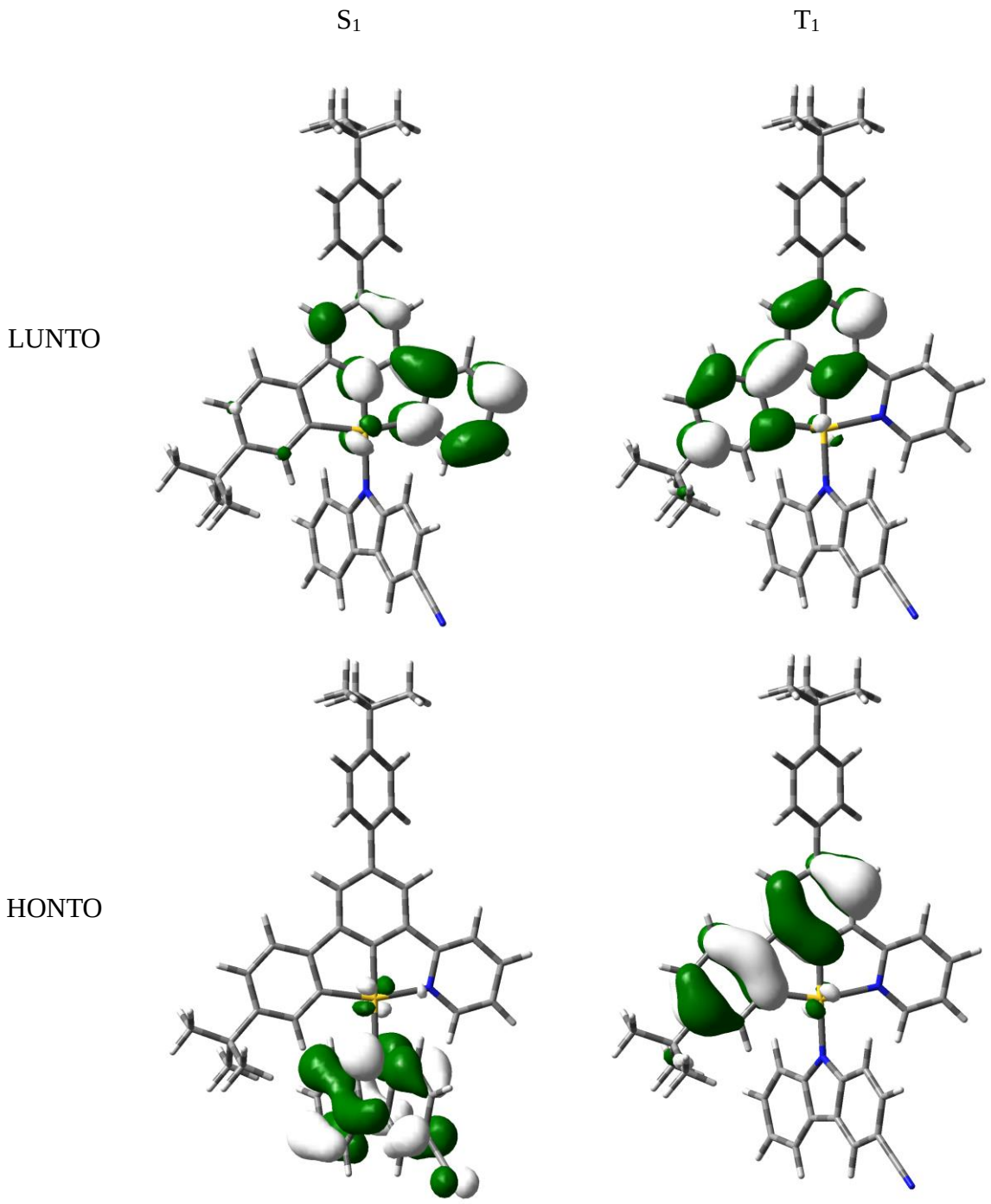

Figure S14. Natural transition orbital (NTO) pairs for the S_1 (left) and T_1 (right) excited states of **1** (Isovalue = 0.03).

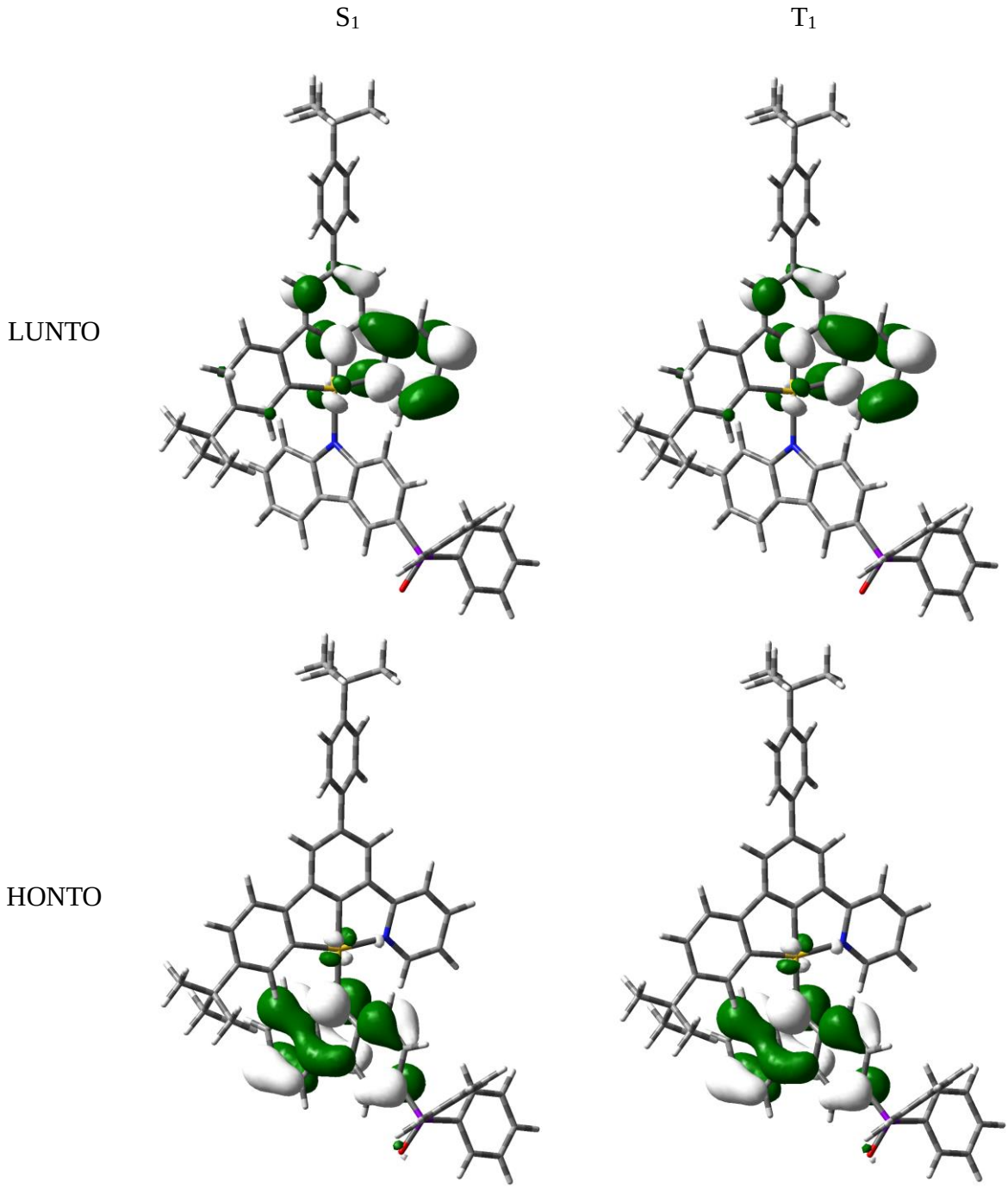

Figure S15. Natural transition orbital (NTO) pairs for the S_1 (left) and T_1 (right) excited states of **2** (Isovalue = 0.03).

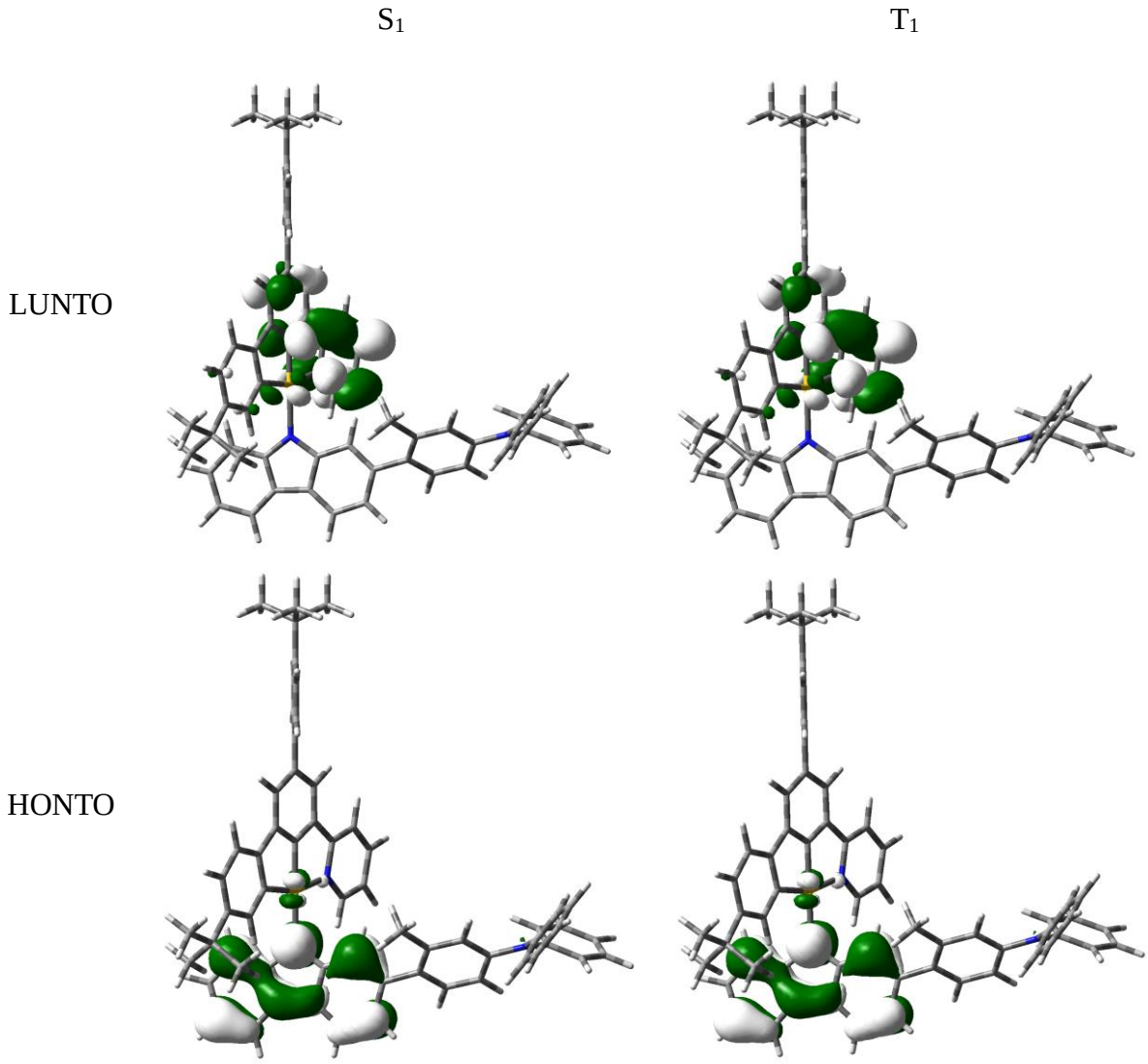

Figure S16. Natural transition orbital (NTO) pairs for the S_1 (left) and T_1 (right) excited states of **6** (Isovalue = 0.03).

Table S4. Cartesian coordinates of the optimized ground-state geometry of **1**.

C	-1.60347	0.952585	-0.11175
C	-1.01034	-0.28297	0.15245
C	-1.73176	-1.45772	0.337523
C	-3.12799	-1.39269	0.252948
C	-3.76007	-0.16858	-0.00573
C	-2.99419	0.999754	-0.18532
C	-0.60672	2.022363	-0.26386
C	0.74255	1.597332	-0.13075
C	1.780721	2.500041	-0.25643
C	1.534031	3.864448	-0.50236
C	0.205481	4.272109	-0.63213
C	-0.85222	3.366773	-0.51783
H	-3.73698	-2.28569	0.360269
H	-3.50634	1.942057	-0.36106
H	2.801201	2.148245	-0.14781
H	-0.02769	5.313701	-0.8244
H	-1.87387	3.723054	-0.62523
Au	0.946861	-0.37189	0.255949
C	5.776482	-2.51916	-1.98132
C	4.408641	-2.6718	-2.31133
C	3.425885	-2.03137	-1.5813
C	3.810995	-1.22658	-0.49675
C	5.191304	-1.05984	-0.16713
C	6.16971	-1.70851	-0.90944
H	4.137564	-3.29971	-3.15398
H	2.378086	-2.14361	-1.84651
H	7.223134	-1.59541	-0.67141
C	3.857912	0.127751	1.249138
C	3.517518	0.985406	2.301706
C	4.545805	1.539398	3.052351
C	5.893855	1.249166	2.777465
C	6.235686	0.394787	1.738178
C	5.217565	-0.16977	0.964477
H	2.477135	1.219204	2.509878
H	4.302301	2.213142	3.869225
H	6.672606	1.699645	3.385578
H	7.278018	0.171864	1.525624
C	6.762838	-3.19906	-2.75403
N	3.018021	-0.52034	0.364082
N	7.565394	-3.75776	-3.38523
C	-0.9169	-2.65424	0.601357
C	-1.41482	-3.93623	0.824536
C	-0.53376	-4.98203	1.072452
H	-2.48479	-4.1091	0.804472
C	1.27763	-3.44254	0.870974
C	0.836156	-4.73815	1.099267
H	-0.9165	-5.98303	1.245708
H	2.330753	-3.17912	0.874833
H	1.552901	-5.52805	1.291137
N	0.429149	-2.44089	0.62654
C	-5.23547	-0.10459	-0.09332
C	-6.04663	-0.8457	0.776488
C	-5.86976	0.695917	-1.04738
C	-7.42996	-0.78423	0.688145
H	-5.58694	-1.45648	1.549193
C	-7.2583	0.753833	-1.13047
H	-5.27104	1.264214	-1.75439
C	-8.073	0.016404	-0.26686
H	-8.02089	-1.36771	1.389086
H	-7.70143	1.383489	-1.89436
C	-9.60031	0.05436	-0.32609
C	-10.147	0.561269	1.018563
H	-11.2421	0.590121	0.994634
H	-9.84832	-0.08588	1.848716
H	-9.78301	1.571741	1.231129
C	-10.1149	0.97779	-1.43317
H	-9.79005	2.012657	-1.28235
H	-9.77952	0.651059	-2.42313
H	-11.2096	0.971536	-1.43571
C	-10.1331	-1.36292	-0.59263
H	-11.228	-1.35401	-0.63215
H	-9.75974	-1.74629	-1.54784
H	-9.83338	-2.06403	0.192127
C	2.721295	4.822453	-0.59484
C	2.284312	6.258587	-0.89273
H	3.165961	6.904604	-0.95263
H	1.753711	6.330933	-1.84815
H	1.635321	6.656976	-0.10566
C	3.665063	4.359612	-1.71696
H	4.521094	5.039181	-1.79239
H	4.055032	3.354093	-1.53285
H	3.14893	4.351067	-2.6826
C	3.476917	4.809688	0.745237
H	2.827584	5.147941	1.559766
H	3.841821	3.809969	1.000901
H	4.341503	5.481134	0.69657

Table S5. Cartesian coordinates of the optimized ground-state geometry of **2**.

C	3.335246	0.920338	0.241718	H	6.597615	-0.37805	2.222697
C	2.456457	0.044602	-0.3983	C	9.113502	-2.10586	0.704157
C	2.818666	-1.2272	-0.83008	H	8.934463	-2.97918	-1.26196
C	4.13591	-1.64763	-0.60828	H	8.894068	-1.10181	2.601358
C	5.048366	-0.79376	0.026616	C	10.55056	-2.58798	0.904444
C	4.643904	0.488186	0.447504	C	11.44187	-1.99683	-0.20012
C	2.688872	2.19448	0.588764	H	12.47578	-2.33699	-0.07416
C	1.317473	2.280413	0.226674	H	11.10947	-2.30127	-1.19712
C	0.587233	3.421137	0.498437	H	11.43494	-0.90263	-0.16226
C	1.181009	4.534058	1.124276	C	11.12065	-2.16423	2.260404
C	2.5282	4.439958	1.477126	H	11.14739	-1.07466	2.366923
C	3.273972	3.28765	1.217311	H	10.54094	-2.57858	3.091997
H	4.462546	-2.6419	-0.89934	H	12.14731	-2.53158	2.356949
H	5.374638	1.142391	0.915724	C	10.5868	-4.12283	0.823571
H	-0.45738	3.459013	0.207878	H	11.61215	-4.48458	0.959018
H	3.022764	5.273839	1.963296	H	9.961154	-4.5689	1.603587
H	4.321304	3.252949	1.507486	H	10.22955	-4.48737	-0.14428
Au	0.608122	0.63305	-0.69413	C	0.333006	5.782583	1.364813
C	-4.9471	-0.3777	0.334167	C	1.117402	6.886604	2.077532
C	-3.75431	-0.99419	0.771689	H	0.469673	7.755745	2.23017
C	-2.51357	-0.52988	0.366983	H	1.473718	6.560724	3.060642
C	-2.462	0.578971	-0.49153	H	1.980063	7.21642	1.488935
C	-3.66081	1.228146	-0.91202	C	-0.8835	5.415175	2.230373
C	-4.89834	0.742253	-0.49845	H	-1.49977	6.30323	2.408906
H	-3.80542	-1.8378	1.45506	H	-1.51589	4.66446	1.747212
H	-1.60118	-1.00305	0.721219	H	-0.56687	5.017741	3.200301
H	-5.82456	1.223463	-0.80229	C	-0.1507	6.324344	0.008521
C	-1.81949	2.258985	-1.7781	H	0.699461	6.605346	-0.62221
C	-1.07676	3.197665	-2.50474	H	-0.745	5.586479	-0.53951
C	-1.76527	4.199383	-3.17613	H	-0.77329	7.213529	0.158418
C	-3.16897	4.27489	-3.14228	P	-6.58422	-0.99581	0.770647
C	-3.9099	3.34218	-2.42932	C	-6.43176	-1.70494	2.439811
C	-3.23887	2.328589	-1.73907	C	-5.96917	-3.00146	2.686601
H	0.008443	3.147749	-2.52615	C	-6.7894	-0.88144	3.512242
H	-1.20551	4.941376	-3.73907	C	-5.84614	-3.46064	3.995563
H	-3.67499	5.071427	-3.67972	H	-5.71848	-3.65843	1.857685
H	-4.99494	3.400311	-2.40264	C	-6.66935	-1.34493	4.818869
N	-1.36123	1.195728	-1.02622	H	-7.17278	0.114607	3.308933
C	1.743695	-1.99409	-1.47977	C	-6.19337	-2.63245	5.061135
C	1.871052	-3.28117	-1.99835	H	-5.48717	-4.46854	4.183186
C	0.776103	-3.89168	-2.5981	H	-6.95053	-0.703	5.648743
H	2.822469	-3.79646	-1.93221	H	-6.10044	-2.9939	6.081362
C	-0.50619	-1.9309	-2.14669	C	-6.91327	-2.41529	-0.32147
C	-0.43499	-3.21072	-2.67855	C	-8.25233	-2.71588	-0.59168
H	0.869907	-4.89468	-3.00284	C	-5.90111	-3.20222	-0.88025
H	-1.4176	-1.34167	-2.17066	C	-8.57554	-3.80172	-1.39982
H	-1.3093	-3.6536	-3.14122	H	-9.03074	-2.08245	-0.17541
N	0.545729	-1.34966	-1.56499	C	-6.22814	-4.29127	-1.68438
C	6.439389	-1.24161	0.257233	H	-4.85821	-2.95536	-0.69848
C	7.129608	-1.98971	-0.70601	C	-7.56402	-4.59265	-1.9423
C	7.111594	-0.93498	1.443636	H	-9.61665	-4.02928	-1.60998
C	8.433244	-2.40967	-0.48388	H	-5.43929	-4.90029	-2.11682
H	6.647158	-2.22141	-1.65204	H	-7.81692	-5.44004	-2.57333
C	8.420058	-1.35855	1.660195	O	-7.66257	0.049145	0.685883

Table S6. Cartesian coordinates of the optimized ground-state geometry of **6**.

C	-3.55844	-0.02573	0.461074
C	-2.59108	0.019159	-0.54445
C	-2.40232	1.116283	-1.37878
C	-3.23224	2.230009	-1.20072
C	-4.22106	2.217637	-0.20729
C	-4.38009	1.088509	0.619657
C	-3.52876	-1.29769	1.198083
C	-2.53194	-2.21195	0.761795
C	-2.3863	-3.44003	1.377648
C	-3.2263	-3.82759	2.439108
C	-4.20311	-2.92347	2.859471
C	-4.35356	-1.67467	2.251781
H	-3.10791	3.122971	-1.80663
H	-5.16713	1.092695	1.369226
H	-1.61892	-4.1192	1.02167
H	-4.86951	-3.18222	3.675166
H	-5.12533	-0.99689	2.608656
Au	-1.41889	-1.53763	-0.77828
C	3.961451	-3.42252	-0.4887
C	3.38442	-2.1404	-0.33753
C	2.010366	-1.9779	-0.51233
C	1.22578	-3.08985	-0.83202
C	1.809507	-4.37947	-0.97225
C	3.187956	-4.53155	-0.79872
H	1.558714	-0.99446	-0.41693
H	3.651278	-5.51005	-0.89781
C	-0.44558	-4.45285	-1.3233
C	-1.69987	-5.01389	-1.59573
C	-1.77378	-6.38277	-1.81726
C	-0.62625	-7.19493	-1.77981
C	0.620581	-6.64354	-1.51646
C	0.721294	-5.26851	-1.28275
H	-2.58992	-4.39069	-1.61679
H	-2.74015	-6.83514	-2.02335
H	-0.71969	-8.26206	-1.95908
H	1.507115	-7.27221	-1.48704
N	-0.13208	-3.13817	-1.05865
C	-1.31919	0.969716	-2.36443
C	-0.94335	1.931519	-3.29993
C	0.099207	1.663767	-4.17916
H	-1.46525	2.88104	-3.33547
C	0.337681	-0.48521	-3.17032
C	0.753843	0.437119	-4.12015
H	0.397883	2.41073	-4.90817
H	0.803126	-1.46	-3.06187
H	1.570584	0.193229	-4.78945
N	-0.65946	-0.22207	-2.32246
C	-5.09681	3.395979	-0.02471
C	-5.58358	4.11508	-1.12464
C	-5.46695	3.833003	1.250215
C	-6.40211	5.221505	-0.94839
H	-5.33879	3.786029	-2.13123
C	-6.28934	4.943453	1.420519
H	-5.08686	3.313945	2.126214
C	-6.77698	5.665607	0.327816
H	-6.76492	5.743923	-1.82956
H	-6.53995	5.246959	2.431215
C	-7.68255	6.888858	0.473859
C	-9.0195	6.616992	-0.23506
H	-9.67944	7.486982	-0.14445
H	-8.88012	6.413313	-1.30102
H	-9.52755	5.754765	0.209021
C	-7.97448	7.222574	1.938996
H	-8.48879	6.400496	2.447846
H	-7.05845	7.45276	2.49325
H	-8.62361	8.10243	1.991904
C	-7.00007	8.105726	-0.17194
H	-7.6397	8.990685	-0.08085
H	-6.04512	8.322289	0.317948
H	-6.80371	7.944216	-1.23617
C	-3.03853	-5.21237	3.058021
C	-4.00226	-5.46253	4.220229
H	-3.82726	-6.4613	4.632737
H	-3.85818	-4.73843	5.029325
H	-5.04781	-5.41672	3.897531
C	-1.59961	-5.34651	3.583195
H	-1.45348	-6.33594	4.030513
H	-0.86178	-5.2318	2.783534
H	-1.39091	-4.591	4.347849
C	-3.28783	-6.27868	1.977467
H	-4.31222	-6.21153	1.595757
H	-2.60591	-6.16909	1.128378
H	-3.14493	-7.28091	2.397044
H	5.03088	-3.53495	-0.33427
C	4.249499	-0.97603	-0.03236
C	5.404105	-0.77681	-0.80266
C	3.969553	-0.06	1.004749
C	6.265183	0.287056	-0.58298
H	5.62505	-1.48224	-1.59929
C	4.833275	1.017073	1.206483
C	5.978456	1.208005	0.429189
H	7.153869	0.413556	-1.19327
H	4.619973	1.723459	2.004361
N	6.834268	2.306596	0.669559
C	2.782549	-0.20446	1.920737
H	1.891194	0.286779	1.512852
H	2.52264	-1.25388	2.080517
H	2.989797	0.256632	2.890383
C	7.379124	3.021848	-0.41677
C	8.699698	3.488485	-0.37244
C	6.607759	3.272936	-1.55938
C	9.228278	4.19846	-1.44435
H	9.304384	3.29129	0.507249
C	7.151948	3.967781	-2.63342
H	5.582964	2.916832	-1.59705
C	8.462358	4.439786	-2.58354
H	10.2541	4.552573	-1.39238
H	6.539352	4.15303	-3.51147
H	8.881562	4.988094	-3.42166
C	7.138241	2.684294	1.994778
C	7.218031	4.037346	2.349237
C	7.359355	1.709483	2.976467
C	7.523274	4.402214	3.655609
H	7.041052	4.796669	1.593854
C	7.645259	2.084779	4.284071
H	7.301118	0.65985	2.705749
C	7.734263	3.431278	4.632923
H	7.581433	5.45617	3.912945
H	7.813165	1.315559	5.032715
H	7.964675	3.720282	5.653816

Table S7. Cartesian coordinates of the optimized S_1 state geometry of **1**.

C	1.600302	0.931745	0.104663
C	1.023341	-0.31464	-0.13898
C	1.741174	-1.50867	-0.31576
C	3.143723	-1.39976	-0.22741
C	3.759767	-0.16952	0.014884
C	2.988304	1.00386	0.180996
C	0.59824	1.999331	0.239494
C	-0.7473	1.557964	0.112465
C	-1.78118	2.472566	0.234571
C	-1.54002	3.841428	0.463123
C	-0.21348	4.255468	0.578867
C	0.843591	3.34626	0.472769
H	3.764289	-2.28688	-0.32287
H	3.488678	1.954974	0.338043
H	-2.80779	2.129237	0.150325
H	0.02015	5.299834	0.755542
H	1.865917	3.703408	0.571718
Au	-0.91981	-0.43425	-0.25521
C	-5.86292	-2.31686	2.054129
C	-4.51395	-2.49981	2.400241
C	-3.50601	-1.93195	1.630487
C	-3.88263	-1.18103	0.514449
C	-5.24843	-0.99413	0.159092
C	-6.24443	-1.55743	0.923549
H	-4.26484	-3.09021	3.27448
H	-2.45925	-2.06694	1.880734
H	-7.2949	-1.43421	0.682878
C	-3.84053	0.062746	-1.30444
C	-3.41853	0.846223	-2.39185
C	-4.39911	1.391113	-3.21146
C	-5.75575	1.16385	-2.95448
C	-6.1822	0.380843	-1.86386
C	-5.22387	-0.16821	-1.03971
H	-2.362	1.022296	-2.56231
H	-4.1108	2.004722	-4.05778
H	-6.50083	1.604322	-3.60883
H	-7.24114	0.224783	-1.68484
C	-6.87974	-2.9105	2.861003
N	-3.05265	-0.54142	-0.37265
N	-7.71198	-3.39116	3.514342
C	0.944462	-2.68306	-0.55725
C	1.413953	-3.98258	-0.7494
C	0.548323	-5.03564	-0.98391
H	2.485953	-4.15451	-0.71137
C	-1.28412	-3.47853	-0.83776
C	-0.84966	-4.76144	-1.03159
H	0.923846	-6.04164	-1.13056
H	-2.34058	-3.23361	-0.87235
H	-1.57292	-5.54617	-1.2224
N	-0.44586	-2.43485	-0.59664
C	5.235161	-0.09287	0.103253
C	6.057117	-0.84909	-0.74403
C	5.864437	0.737494	1.035749
C	7.439951	-0.77672	-0.65308
H	5.603197	-1.48404	-1.5003
C	7.25255	0.808329	1.121334
H	5.258916	1.321	1.724322
C	8.075635	0.053575	0.281169
H	8.036551	-1.37562	-1.33643
H	7.688541	1.462414	1.869005
C	9.602728	0.103221	0.343457
C	10.15147	0.576743	-1.0124
H	11.24651	0.612501	-0.98711
H	9.857745	-0.09408	-1.82536
H	9.781909	1.578936	-1.25308
C	10.1083	1.05986	1.426301
H	9.776183	2.087804	1.246472
H	9.771141	0.758078	2.423576
H	11.20312	1.061345	1.432604
C	10.14508	-1.30218	0.650266
H	11.24007	-1.28578	0.692167
H	9.771152	-1.6615	1.614598
H	9.850885	-2.02643	-0.11531
C	-2.72997	4.796982	0.564122
C	-2.29321	6.243005	0.81083
H	-3.17538	6.888311	0.874881
H	-1.7392	6.343243	1.750035
H	-1.66386	6.620013	-0.00217
C	-3.63764	4.361593	1.72621
H	-4.49797	5.035387	1.8093
H	-4.0212	3.346563	1.583373
H	-3.09216	4.384555	2.675227
C	-3.52844	4.750927	-0.7498
H	-2.90344	5.05864	-1.59476
H	-3.90699	3.745906	-0.96142
H	-4.38836	5.428285	-0.69581

Table S8. Cartesian coordinates of the optimized S_1 state geometry of **2**.

C	3.329721	0.904493	0.235069
C	2.483753	0.002765	-0.41057
C	2.865868	-1.27217	-0.85869
C	4.206636	-1.63239	-0.61496
C	5.084956	-0.75683	0.02847
C	4.648935	0.518441	0.455884
C	2.651854	2.162963	0.580714
C	1.280526	2.210236	0.208071
C	0.532524	3.341056	0.493825
C	1.09658	4.46404	1.130178
C	2.444289	4.400657	1.482802
C	3.212813	3.263334	1.215859
H	4.566705	-2.61563	-0.90637
H	5.356102	1.195391	0.926375
H	-0.51739	3.366887	0.21837
H	2.920968	5.241492	1.975104
H	4.260196	3.247076	1.507924
Au	0.633689	0.529686	-0.73401
C	-4.96082	-0.35843	0.378763
C	-3.78488	-0.98003	0.814377
C	-2.53651	-0.5466	0.369145
C	-2.50353	0.534231	-0.51249
C	-3.6905	1.187412	-0.94233
C	-4.91875	0.747105	-0.4974
H	-3.83883	-1.80674	1.516075
H	-1.61915	-1.02758	0.692126
H	-5.84724	1.228548	-0.79079
C	-1.819	2.139857	-1.8602
C	-1.02599	3.023002	-2.61329
C	-1.67548	4.019537	-3.32982
C	-3.07082	4.133303	-3.29681
C	-3.86835	3.2511	-2.54337
C	-3.24248	2.255075	-1.82477
H	0.054301	2.926476	-2.61065
H	-1.09575	4.722367	-3.91809
H	-3.55177	4.923812	-3.86369
H	-4.94774	3.363492	-2.53143
N	-1.38964	1.115464	-1.07495
C	1.831225	-2.0411	-1.50058
C	1.950069	-3.33386	-2.01077
C	0.882327	-3.97294	-2.61538
H	2.909276	-3.83642	-1.92334
C	-0.44578	-2.00554	-2.20198
C	-0.35522	-3.27197	-2.71246
H	0.985796	-4.97804	-3.00744
H	-1.37079	-1.44186	-2.26263
H	-1.22185	-3.71862	-3.18676
N	0.592238	-1.36843	-1.59704
C	6.486005	-1.1687	0.269322
C	7.202927	-1.90846	-0.68157
C	7.147655	-0.83431	1.454882
C	8.515135	-2.29519	-0.44843
H	6.730274	-2.16202	-1.62681
C	8.465419	-1.22256	1.682921
H	6.615733	-0.28107	2.224454
C	9.182559	-1.96282	0.739154
H	9.033534	-2.86093	-1.21838
H	8.927854	-0.94343	2.623774
C	10.63025	-2.40736	0.951222
C	11.51341	-1.80657	-0.15458
H	12.55494	-2.12034	-0.0211
H	11.19229	-2.12855	-1.14977
H	11.47956	-0.71248	-0.12792
C	11.18326	-1.95572	2.30531
H	11.18184	-0.86473	2.400383
H	10.60887	-2.37506	3.138106
H	12.21831	-2.29655	2.411231
C	10.70594	-3.94149	0.887102
H	11.73934	-4.27702	1.030433
H	10.0876	-4.39444	1.669009
H	10.36111	-4.32452	-0.07808
C	0.216333	5.686909	1.392689
C	0.982854	6.814808	2.087571
H	0.314731	7.666179	2.253587
H	1.369016	6.50011	3.062765
H	1.824297	7.165905	1.481
C	-0.96581	5.282663	2.288801
H	-1.60895	6.148604	2.482704
H	-1.58179	4.507244	1.823048
H	-0.61083	4.897828	3.250401
C	-0.31984	6.220699	0.053402
H	0.504304	6.517926	-0.6037
H	-0.91589	5.470097	-0.47512
H	-0.9567	7.096762	0.221178
P	-6.62254	-0.9181	0.876275
C	-6.41862	-1.66273	2.516867
C	-6.02617	-2.99132	2.7104
C	-6.65607	-0.83707	3.621076
C	-5.85335	-3.48226	4.001728
H	-5.86949	-3.64658	1.857732
C	-6.48639	-1.33435	4.90931
H	-6.9854	0.185532	3.459834
C	-6.08048	-2.65419	5.099291
H	-5.54912	-4.51401	4.150615
H	-6.67366	-0.69316	5.765503
H	-5.94802	-3.041	6.105542
C	-7.03491	-2.26613	-0.26602
C	-8.38837	-2.43439	-0.57669
C	-6.07977	-3.12249	-0.82468
C	-8.78378	-3.46262	-1.4268
H	-9.11864	-1.74745	-0.15834
C	-6.48113	-4.15156	-1.67193
H	-5.02301	-2.98194	-0.61343
C	-7.83162	-4.32298	-1.97043
H	-9.83484	-3.59029	-1.66825
H	-5.73804	-4.81433	-2.10527
H	-8.14143	-5.12441	-2.63485
O	-7.61858	0.205621	0.849806

Table S9. Cartesian coordinates of the optimized S_1 state geometry of **6**.

C	-3.52203	-0.10971	0.50169
C	-2.61749	-0.04765	-0.55821
C	-2.53101	1.013229	-1.4748
C	-3.4387	2.073002	-1.27493
C	-4.36118	2.046667	-0.2259
C	-4.40669	0.952409	0.668502
C	-3.37953	-1.34282	1.290671
C	-2.35377	-2.21477	0.832725
C	-2.11483	-3.40213	1.505663
C	-2.87374	-3.78615	2.628349
C	-3.87864	-2.92045	3.058989
C	-4.12727	-1.71147	2.401528
H	-3.41127	2.942179	-1.92694
H	-5.15142	0.93837	1.45903
H	-1.32367	-4.05901	1.157569
H	-4.48816	-3.17466	3.919533
H	-4.9165	-1.05847	2.766699
Au	-1.37473	-1.52969	-0.8105
C	4.064822	-3.32065	-0.4878
C	3.471873	-2.056	-0.34975
C	2.086821	-1.93306	-0.54223
C	1.350469	-3.07622	-0.8453
C	1.957761	-4.3513	-0.98492
C	3.322686	-4.46966	-0.80762
H	1.595269	-0.96834	-0.48505
H	3.822756	-5.42912	-0.89891
C	-0.30615	-4.44852	-1.32716
C	-1.57495	-4.99268	-1.58376
C	-1.65478	-6.35902	-1.81716
C	-0.50484	-7.15939	-1.79263
C	0.766392	-6.61939	-1.533
C	0.868972	-5.26248	-1.2988
H	-2.45338	-4.35619	-1.58132
H	-2.61889	-6.81476	-2.01512
H	-0.59769	-8.22535	-1.97431
H	1.640328	-7.26287	-1.51348
N	-0.00802	-3.14894	-1.05213
C	-1.51736	0.876754	-2.48835
C	-1.21408	1.796538	-3.49243
C	-0.21155	1.55442	-4.41437
H	-1.78611	2.719129	-3.53676
C	0.195175	-0.55495	-3.32357
C	0.511963	0.329964	-4.31827
H	0.016914	2.276913	-5.18931
H	0.72249	-1.4977	-3.22168
H	1.302867	0.084657	-5.01802
N	-0.78442	-0.32858	-2.40821
C	-5.29834	3.177897	-0.04526
C	-5.88272	3.823894	-1.14377
C	-5.6367	3.644741	1.228606
C	-6.75724	4.887062	-0.9686
H	-5.66517	3.469916	-2.14803
C	-6.51692	4.710298	1.399181
H	-5.18541	3.182807	2.102794
C	-7.09877	5.359244	0.3068
H	-7.19177	5.35163	-1.85008
H	-6.73805	5.037369	2.409684
C	-8.06965	6.531735	0.451951
C	-9.41949	6.154996	-0.18028
H	-10.1265	6.987525	-0.0903
H	-9.31691	5.917	-1.2433
H	-9.85292	5.282424	0.319372
C	-8.31333	6.905221	1.916358
H	-8.75166	6.074317	2.479186
H	-7.38791	7.210019	2.416384
H	-9.01178	7.746699	1.96923
C	-7.49416	7.761151	-0.26966
H	-8.18185	8.609885	-0.18126
H	-6.53277	8.052945	0.16564
H	-7.33608	7.568744	-1.3351
C	-2.56792	-5.12242	3.306607
C	-3.47843	-5.38457	4.508592
H	-3.22362	-6.34879	4.960494
H	-3.36239	-4.61502	5.279005
H	-4.53311	-5.42279	4.216415
C	-1.11003	-5.12563	3.795119
H	-0.87436	-6.07923	4.281218
H	-0.40519	-4.98884	2.969161
H	-0.94075	-4.32154	4.518763
C	-2.76637	-6.26137	2.29196
H	-3.79975	-6.28263	1.930055
H	-2.10953	-6.15223	1.423245
H	-2.5474	-7.22862	2.758695
H	5.134492	-3.41281	-0.3266
C	4.302578	-0.86863	-0.04989
C	5.467974	-0.65839	-0.79925
C	3.973876	0.055514	0.964657
C	6.298087	0.42774	-0.5783
H	5.722064	-1.36535	-1.58459
C	4.811777	1.149382	1.172954
C	5.971655	1.356488	0.417544
H	7.194229	0.564111	-1.17432
H	4.5609	1.862091	1.953141
N	6.793683	2.471208	0.658278
C	2.76163	-0.09423	1.846288
H	1.872056	0.360228	1.394828
H	2.52475	-1.14342	2.042454
H	2.924149	0.404104	2.80532
C	7.441656	3.121927	-0.4167
C	8.768561	3.548605	-0.2857
C	6.763035	3.35401	-1.61923
C	9.399384	4.201214	-1.3389
H	9.296017	3.367205	0.645713
C	7.408637	3.990463	-2.67336
H	5.731055	3.032049	-1.71943
C	8.727244	4.42176	-2.53976
H	10.42906	4.527372	-1.22267
H	6.869501	4.163666	-3.6004
H	9.225315	4.925663	-3.36246
C	6.971795	2.957842	1.973574
C	6.966226	4.335274	2.223246
C	7.163809	2.069781	3.039019
C	7.156457	4.811487	3.515605
H	6.81406	5.024645	1.398537
C	7.334014	2.554997	4.330685
H	7.175414	1.001506	2.84586
C	7.336105	3.926783	4.577369
H	7.149539	5.882989	3.694171
H	7.480763	1.854004	5.147516
H	7.47663	4.302299	5.586345

Table S10. Cartesian coordinates of the optimized T_1 state geometry of **1**.

C	1.593408	0.999649	0.139185	H	2.481645	-4.087	-0.80309
C	0.98788	-0.28204	-0.1389	C	-1.28526	-3.43904	-0.87965
C	1.70725	-1.44635	-0.3218	C	-0.83492	-4.73358	-1.11238
C	3.121221	-1.38226	-0.22831	H	0.924262	-5.96818	-1.2588
C	3.7733	-0.12141	0.036054	H	-2.34009	-3.18248	-0.88755
C	3.02988	1.034207	0.209576	H	-1.5471	-5.52601	-1.31051
C	0.645927	2.01536	0.286131	N	-0.44552	-2.43529	-0.62671
C	-0.75727	1.590982	0.138079	C	5.245174	-0.08582	0.114817
C	-1.77644	2.49738	0.262227	C	6.038705	-0.90495	-0.7035
C	-1.52493	3.874997	0.513829	C	5.906369	0.767477	1.006487
C	-0.16568	4.286457	0.663383	C	7.423228	-0.85744	-0.63533
C	0.883377	3.406886	0.560964	H	5.565687	-1.56545	-1.42535
H	3.727736	-2.27802	-0.30676	C	7.295324	0.809237	1.070275
H	3.539988	1.979658	0.368378	H	5.325448	1.389399	1.682141
H	-2.80015	2.156822	0.146874	C	8.090083	-0.00029	0.252388
H	0.052932	5.329479	0.865355	H	7.996927	-1.50076	-1.29714
H	1.903457	3.759505	0.684508	H	7.756439	1.48187	1.785362
Au	-0.95943	-0.36571	-0.24951	C	9.617976	0.015426	0.295117
C	-5.78162	-2.5462	1.965842	C	10.15891	0.413125	-1.08816
C	-4.41349	-2.69119	2.298501	H	11.25449	0.424253	-1.07662
C	-3.4334	-2.03978	1.574731	H	9.840494	-0.28748	-1.86594
C	-3.82142	-1.23115	0.494043	H	9.809823	1.411659	-1.37066
C	-5.20197	-1.07256	0.161507	C	10.15905	1.008596	1.326668
C	-6.17775	-1.7323	0.897501	H	9.848319	2.034808	1.103987
H	-4.14021	-3.32229	3.138057	H	9.829788	0.76028	2.341159
H	-2.38523	-2.14621	1.840898	H	11.25342	0.984926	1.318734
H	-7.23132	-1.62537	0.657231	C	10.13038	-1.38749	0.65993
C	-3.87293	0.132156	-1.24445	H	11.22567	-1.39427	0.688874
C	-3.53629	0.99746	-2.29204	H	9.760545	-1.69366	1.643941
C	-4.56659	1.547205	-3.04315	H	9.811276	-2.13884	-0.06868
C	-5.91327	1.245997	-2.7734	C	-2.70407	4.836301	0.584322
C	-6.25148	0.384227	-1.73904	C	-2.26765	6.271922	0.888003
C	-5.23136	-0.17664	-0.96529	H	-3.14848	6.920242	0.931728
H	-2.4969	1.239354	-2.49556	H	-1.75413	6.344675	1.852677
H	-4.32566	2.226102	-3.85656	H	-1.60448	6.668085	0.111739
H	-6.69369	1.693599	-3.38151	C	-3.67213	4.379277	1.689985
H	-7.29269	0.152468	-1.5304	H	-4.5276	5.061641	1.744158
C	-6.76521	-3.23723	2.732128	H	-4.06146	3.374205	1.502436
N	-3.03095	-0.51435	-0.36014	H	-3.17601	4.374233	2.665978
N	-7.56558	-3.80484	3.35817	C	-3.43851	4.824893	-0.76939
C	0.904246	-2.64187	-0.59564	H	-2.77556	5.161907	-1.5733
C	1.410796	-3.92045	-0.82463	H	-3.80243	3.826239	-1.0305
C	0.535521	-4.97018	-1.08161	H	-4.3019	5.498818	-0.73356

Table S11. Cartesian coordinates of the optimized T_1 state geometry of **2**.

C	3.338129	0.911077	0.219507
C	2.477593	0.011058	-0.41017
C	2.844447	-1.27363	-0.84501
C	4.183501	-1.64419	-0.60744
C	5.075768	-0.76937	0.017065
C	4.655233	0.515474	0.432877
C	2.673483	2.176553	0.563787
C	1.297747	2.230368	0.209168
C	0.560117	3.366241	0.501877
C	1.139548	4.488648	1.125372
C	2.491998	4.419551	1.458329
C	3.249782	3.276564	1.185903
H	4.530994	-2.63511	-0.88785
H	5.372675	1.190927	0.889738
H	-0.49382	3.396736	0.243024
H	2.980422	5.259782	1.939989
H	4.300914	3.255008	1.463788
Au	0.628385	0.548897	-0.71745
C	-4.95919	-0.36218	0.385624
C	-3.78219	-0.99017	0.809432
C	-2.53468	-0.54695	0.371974
C	-2.50335	0.548721	-0.49146
C	-3.69119	1.208505	-0.90802
C	-4.91883	0.759235	-0.46983
H	-3.83483	-1.82979	1.495743
H	-1.61648	-1.03175	0.686827
H	-5.84787	1.245368	-0.75355
C	-1.82269	2.179842	-1.81162
C	-1.0331	3.074168	-2.55415
C	-1.68561	4.081125	-3.25365
C	-3.08085	4.192872	-3.21562
C	-3.87498	3.297923	-2.47433
C	-3.2456	2.292112	-1.77196
H	0.047226	2.977893	-2.55735
H	-1.10788	4.79309	-3.83288
H	-3.56418	4.990982	-3.76971
H	-4.95468	3.407068	-2.4593
N	-1.39024	1.14111	-1.04476
C	1.799472	-2.03868	-1.47315
C	1.908246	-3.3318	-1.98597
C	0.833661	-3.96416	-2.5846
H	2.865644	-3.83901	-1.90624
C	-0.47984	-1.98853	-2.16373
C	-0.39953	-3.25513	-2.67588
H	0.929533	-4.96888	-2.97961
H	-1.40125	-1.41898	-2.22174
H	-1.27098	-3.69532	-3.14739
N	0.563221	-1.36021	-1.55866
C	6.474551	-1.19186	0.251492
C	7.175177	-1.95317	-0.69463
C	7.150501	-0.84664	1.425906
C	8.485395	-2.34997	-0.46753
H	6.691455	-2.21577	-1.63175
C	8.466179	-1.24521	1.647881
H	6.631468	-0.27659	2.191986
C	9.167036	-2.00687	0.708897
H	8.990903	-2.93244	-1.23355
H	8.940038	-0.95693	2.580244
C	10.61188	-2.46337	0.914685
C	11.49099	-1.88953	-0.20853
H	12.53037	-2.21215	-0.07946
H	11.15745	-2.22384	-1.19552
H	11.46882	-0.79486	-0.19901
C	11.18221	-1.99642	2.256337
H	11.19287	-0.90412	2.334263
H	10.61145	-2.39671	3.100915
H	12.21465	-2.3463	2.358004
C	10.6707	-3.99905	0.874148
H	11.70179	-4.34336	1.013285
H	10.05493	-4.43299	1.668766
H	10.31282	-4.39346	-0.08165
C	0.26973	5.716953	1.397171
C	1.052706	6.843197	2.076244
H	0.391559	7.698555	2.24951
H	1.45222	6.529922	3.046503
H	1.886461	7.187894	1.455547
C	-0.90042	5.321821	2.312894
H	-1.53597	6.191769	2.513721
H	-1.52756	4.548092	1.859414
H	-0.53254	4.938401	3.270202
C	-0.28447	6.249054	0.064604
H	0.530829	6.539071	-0.60662
H	-0.89325	5.500168	-0.4516
H	-0.91341	7.129475	0.23928
P	-6.61983	-0.93495	0.871153
C	-6.41584	-1.71212	2.496634
C	-6.01719	-3.04251	2.66342
C	-6.66009	-0.91088	3.617207
C	-5.84501	-3.55946	3.944626
H	-5.85513	-3.67899	1.797627
C	-6.49106	-1.43414	4.895217
H	-6.99413	0.113224	3.476505
C	-6.07902	-2.75562	5.058658
H	-5.53593	-4.59256	4.072711
H	-6.68363	-0.81191	5.764128
H	-5.9471	-3.1627	6.056955
C	-7.02774	-2.26115	-0.29812
C	-8.38099	-2.43021	-0.60936
C	-6.06931	-3.10048	-0.87662
C	-8.77282	-3.4426	-1.47986
H	-9.11403	-1.75606	-0.17533
C	-6.46709	-4.11382	-1.74429
H	-5.01283	-2.95849	-0.66487
C	-7.8173	-4.28631	-2.04337
H	-9.82372	-3.57087	-1.7217
H	-5.72143	-4.76336	-2.193
H	-8.12434	-5.07538	-2.72369
O	-7.6189	0.186371	0.866478

Table S12. Cartesian coordinates of the optimized T_1 state geometry of **6**.

C	-3.5453	-0.09354	0.475777
C	-2.61243	-0.02677	-0.55952
C	-2.48433	1.051976	-1.45062
C	-3.37973	2.122592	-1.25291
C	-4.33137	2.089742	-0.23078
C	-4.41802	0.978363	0.639667
C	-3.43847	-1.34019	1.248313
C	-2.40975	-2.21641	0.805697
C	-2.19962	-3.41393	1.470318
C	-2.99212	-3.80488	2.567113
C	-4.0006	-2.93543	2.981588
C	-4.21945	-1.71575	2.333789
H	-3.31921	3.005206	-1.8843
H	-5.18401	0.960632	1.409545
H	-1.40476	-4.0737	1.136647
H	-4.63551	-3.19467	3.82202
H	-5.01134	-1.05918	2.686583
Au	-1.3812	-1.51953	-0.8033
C	4.040433	-3.35337	-0.47202
C	3.457865	-2.08371	-0.33464
C	2.074096	-1.94935	-0.52755
C	1.328758	-3.08595	-0.8335
C	1.925566	-4.36577	-0.97268
C	3.289189	-4.49594	-0.79286
H	1.590014	-0.98098	-0.46843
H	3.781019	-5.45974	-0.88305
C	-0.33835	-4.44566	-1.31854
C	-1.60978	-4.97921	-1.58233
C	-1.69933	-6.34472	-1.81858
C	-0.55586	-7.15389	-1.79167
C	0.718392	-6.62382	-1.52693
C	0.83004	-5.26813	-1.28891
H	-2.48314	-4.33578	-1.58333
H	-2.66627	-6.79232	-2.02136
H	-0.65604	-8.21865	-1.97655
H	1.587829	-7.27338	-1.50741
N	-0.03062	-3.14749	-1.04192
C	-1.4499	0.918114	-2.44248
C	-1.12205	1.843653	-3.43399
C	-0.10848	1.599371	-4.34269
H	-1.68528	2.771551	-3.47973
C	0.256927	-0.52539	-3.2672
C	0.59839	0.36523	-4.2486
H	0.138177	2.325554	-5.10856
H	0.770757	-1.47577	-3.16878
H	1.396078	0.116835	-4.9395
N	-0.72906	-0.29399	-2.35995
C	-5.2554	3.231941	-0.05241
C	-5.79856	3.909497	-1.15308
C	-5.62229	3.678044	1.221024
C	-6.66117	4.982698	-0.98023
H	-5.55834	3.572566	-2.15803
C	-6.49029	4.753949	1.389151
H	-5.20304	3.191247	2.097668
C	-7.0311	5.434229	0.294746
H	-7.0635	5.472023	-1.86359
H	-6.73465	5.063915	2.399697
C	-7.98722	6.619103	0.437179
C	-9.32442	6.277406	-0.24019
H	-10.0205	7.119384	-0.15269
H	-9.19565	6.059448	-1.30465
H	-9.78552	5.40207	0.228919
C	-8.26626	6.966508	1.901694
H	-8.73327	6.131504	2.434589
H	-7.35067	7.24595	2.433606
H	-8.95266	7.817963	1.952631
C	-7.37233	7.853458	-0.2423
H	-8.04875	8.711346	-0.15529
H	-6.41906	8.120508	0.225516
H	-7.18746	7.680353	-1.30675
C	-2.71656	-5.15202	3.236857
C	-3.6605	-5.41955	4.411572
H	-3.42638	-6.39138	4.858317
H	-3.55755	-4.66024	5.193917
H	-4.70753	-5.44442	4.091711
C	-1.27205	-5.17526	3.763061
H	-1.0584	-6.13673	4.243816
H	-0.54451	-5.03603	2.957458
H	-1.11402	-4.38132	4.500328
C	-2.8992	-6.27686	2.203721
H	-3.92291	-6.28373	1.814763
H	-2.21889	-6.1639	1.353794
H	-2.70175	-7.25167	2.664303
H	5.109059	-3.45449	-0.30918
C	4.298377	-0.90319	-0.03489
C	5.465633	-0.70319	-0.78417
C	3.977076	0.024542	0.978709
C	6.304616	0.37627	-0.56397
H	5.714043	-1.41291	-1.56884
C	4.823847	1.111766	1.186144
C	5.985509	1.308623	0.430834
H	7.202002	0.504765	-1.15988
H	4.578625	1.827297	1.965557
N	6.816596	2.416942	0.670595
C	2.763406	-0.11437	1.860099
H	1.877885	0.347467	1.408113
H	2.51757	-1.16142	2.056677
H	2.929917	0.38304	2.818925
C	7.468496	3.06225	-0.40522
C	8.798625	3.479238	-0.27557
C	6.790708	3.298525	-1.60741
C	9.433418	4.12649	-1.32969
H	9.325479	3.294577	0.655545
C	7.440171	3.929499	-2.66247
H	5.756319	2.984079	-1.70664
C	8.762017	4.351182	-2.5302
H	10.46557	4.445118	-1.21446
H	6.901603	4.10602	-3.58921
H	9.263154	4.850845	-3.35362
C	6.999544	2.902423	1.985609
C	7.005569	4.279916	2.235007
C	7.1847	2.013066	3.051199
C	7.200459	4.754824	3.527153
H	6.858698	4.970364	1.410239
C	7.359652	2.497146	4.342656
H	7.187256	0.944682	2.85831
C	7.37331	3.868919	4.589042
H	7.202542	5.826393	3.705458
H	7.500978	1.795129	5.159567
H	7.517505	4.243483	5.597855

Table S13. Molecular orientation parameters of **6** and [Au{4-^{t}BuC^C(4-^{t}BuC$_6$H$_4$)^N}(Cbz)].

Complex	Order Parameter (S)	θ^a / °	Θ^b	(h:v)^b
6	−0.16	61.6	0.77	0.77:0.23
[Au{4-^{t}BuC^C(4-^{t}BuC$_6$H$_4$)^N}(Cbz)]	−0.04	56.4	0.69	0.69:0.31

[a] θ represents the angle between the normal of a substrate and the transition dipole moment vector (TDMV) and is calculated by the equation $S = \frac{1}{2}\langle 3\cos^2\theta - 1\rangle$, with the bracketed values $\langle ... \rangle$ indicating an ensemble average of $\langle\cos^2\theta\rangle$. From ref. 2.

[b] Θ represents the ratio of the horizontal dipole to the total dipole of the emitters and is obtained by the equation $\langle\Theta : 1 - \Theta\rangle = \langle\sin^2\theta\rangle : \langle\cos^2\theta\rangle$ = h:v. From ref. 3 and 4.

Table S14. Key parameters of the solution-processed OLEDs based on **1**–**6**.

Complex	Conc. / wt%	CE[a] / cd A^{-1}	PE[b] / lm W^{-1}	EQE[c] / %	λ_{max}[d] / nm	CIE[e] / *x*, *y*
1	5	15.4	0.9	1.2	496, 524	0.26,0.53
	10	17.7	7.9	5.8	500, 528	0.27,0.54
	15	20.2	10.6	6.5	500, 528	0.28,0.56
	20	26.2	13.7	8.4	500, 528	0.29,0.56
2	5	11.5	3.1	3.7	500	0.25,0.56
	10	29.7	10.4	9.3	520	0.27,0.57
	15	35.9	16.1	11.3	520	0.27,0.57
	20	38.0	17.1	11.7	520	0.29,0.58
3	5	8.4	1.3	2.9	568	0.46,0.52
	10	13.0	4.2	5.1	580	0.50,0.49
	15	13.3	4.2	5.3	588	0.51,0.48
	20	15.4	6.3	6.1	584	0.51,0.48
4	5	11.4	2.0	3.6	556	0.41,0.54
	10	20.2	6.5	6.7	564	0.45,0.53
	15	26.2	10.4	9.1	572	0.47,0.51
	20	27.7	11.4	10.0	576	0.49,0.50
5	5	9.7	2.1	3.0	532	0.36,0.56
	10	27.2	9.7	8.4	548	0.40,0.55
	15	32.7	14.4	10.2	556	0.42,0.55
	20	36.6	18.7	11.4	560	0.44,0.54
6	5	12.7	2.7	3.9	532	0.34,0.56
	10	23.2	6.9	7.0	540	0.38,0.56
	15	31.0	12.1	9.4	552	0.41,0.56
	20	34.8	15.6	10.9	556	0.42,0.55

[a] CE represents maximum current efficiency.

[b] PE represents maximum power efficiency.

[c] EQE represents maximum external quantum efficiency.

[d] λ_{max} represents peak maximum.

[e] CIE coordinates are taken at a current density of 100 cd m^{-2}.

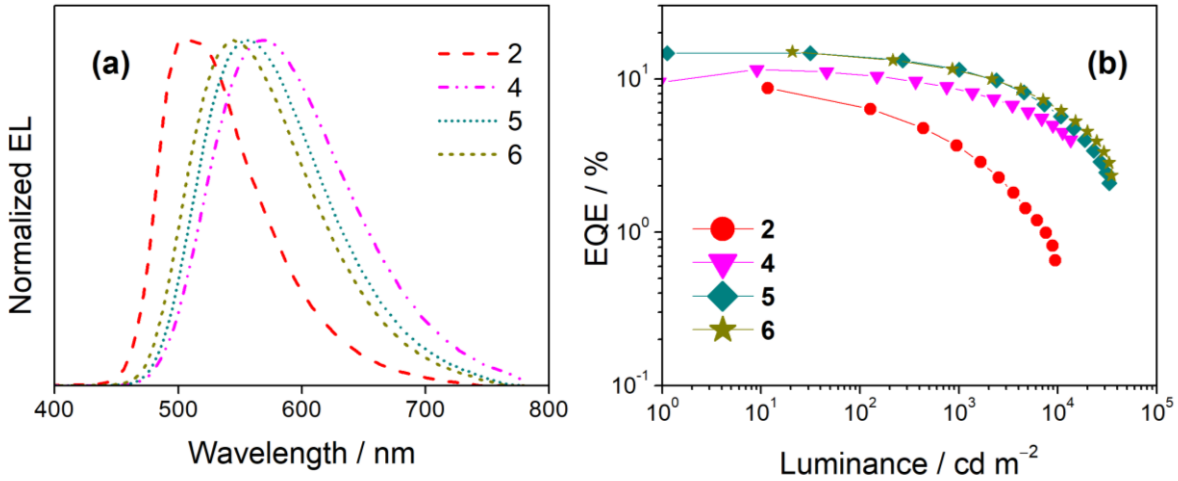

Figure S17. (a) Normalized EL spectra and (b) EQEs of the vacuum-deposited OLEDs based on 8 % v/v **2**, **4**, **5**, and **6**.

Table S15. Efficiency roll-off ($\Delta_{roll\text{-}off}$) of the solution-processed devices doped with 20 wt% **1**–**6**.

		L @ 1000 cd m^{-2}		L @ 5000 cd m^{-2}	
Complex	Max. EQE / %	EQE / %	$\Delta_{roll\text{-}off}$ / %	EQE / %	$\Delta_{roll\text{-}off}$ / %
1	8.4	2.9	65	--	--
2	11.7	10.8	8	5.4	54
3	6.1	5.9	3	4.5	26
4	10.0	9.9	1	8.3	17
5	11.4	11.1	3	7.3	36
6	10.9	10.7	2	8.9	18

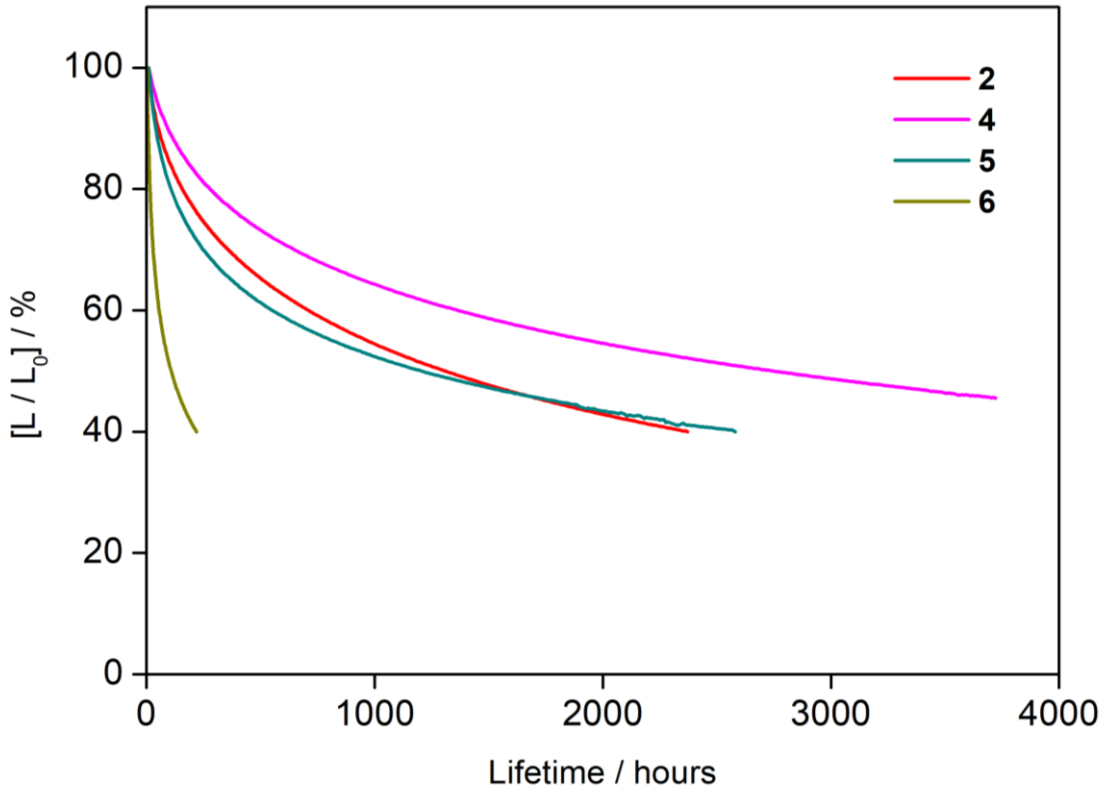

Figure S18. Relative luminance of the vacuum-deposited OLEDs based on 11 % v/v **2**, **4**, **5**, and **6** as a function of operational time.

Table S16. Key parameters of the vacuum-deposited OLEDs based on **2**, **4**, **5** and **6**.

Complex	Conc. / wt%	CE[a] / cd A^{-1}	PE[b] / lm W^{-1}	EQE[c] / %	λ_{max}[d] / nm	CIE (x, y)[e]
2	2	10.2	9.2	3.5	496	0.26,0.51
	5	19.0	17.1	6.4	500	0.27,0.54
	8	26.5	23.8	8.7	508	0.29,0.55
	11	34.8	36.4	11.8	520	0.30,0.56
	14	36.6	38.3	12.0	528	0.33,0.56
4	2	31.6	25.3	10.6	544	0.41,0.54
	5	33.7	30.3	12.2	564	0.45,0.52
	8	30.0	23.6	11.5	572	0.46,0.51
	11	27.7	22.6	10.8	572	0.47,0.51
	14	25.6	21.1	9.8	572	0.46,0.52
5	2	38.6	34.7	12.3	540	0.38,0.55
	5	44.6	46.7	14.6	552	0.42,0.55
	8	43.7	43.9	14.7	556	0.43,0.54
	11	42.6	41.5	14.9	564	0.46,0.53
	14	38.8	36.7	14.2	572	0.46,0.52
6	2	36.7	33.0	11.7	530	0.36,0.56
	5	42.6	38.3	13.6	540	0.39,0.56
	8	46.4	41.6	15.0	544	0.40,0.55
	11	43.1	42.2	14.1	544	0.41,0.55
	14	36.8	38.6	11.8	544	0.41,0.55

[a] CE represents maximum current efficiency.

[b] PE represents maximum power efficiency.

[c] EQE represents maximum external quantum efficiency.

[d] λ_{max} represents peak maximum.

[e] CIE coordinates are taken at a luminance of 100 cd m^{-2}.

Table S17. Lifetime data of the vacuum-deposited OLEDs based on **2**, **4**–**6**.

Complex	L_0 [a] / cd m^{-2}	Lifetime / hours	
		LT_{70} [b] at 100 cd m^{-2}	LT_{50} [c] at 100 cd m^{-2}
2	3314	358	1315
4	4321	652	2760
5	4442	257	1215
6	2110	30	110

[a] L_0 is defined as the initial luminance.

[b] LT_{70} is defined as the operational lifetime at 70 % of initial luminance.

[c] LT_{50} is defined as the operational lifetime at 50 % of initial luminance.

Table S18. TADF OLEDs with similar CIE coordinates as **6**.

Emitter	CE[a] / cd A^{-1}	PE[b] / lm W^{-1}	EQE[c] / %	λ_{max}[d] / nm	CIE (x, y)[e]
PyCN-TC[5]	26.7	3.6[f]	8.1	546	0.40,0.55
PXZDSO2[6]	49.3	38.5	16.7	560	0.44,0.54
TTPPCuBr[7]	32.7	28.8	12.4	584	0.47,0.50
TTPPCuI[7]	40.8	35.9	16.3	584	0.48,0.49

[a] CE represents maximum current efficiency.

[b] PE represents maximum power efficiency.

[c] EQE represents maximum external quantum efficiency.

[d] λ_{max} represents peak maximum.

[e] CIE coordinates are taken at a luminance of 100 cd m^{-2}.

[f] PE are taken at a luminance of 100 cd m^{-2}.

Materials and reagents. Potassium tetrachloroaurate(III) was purchased from Strem Chemicals Inc.. All solvents were purified and distilled using standard procedures before use. All other reagents were of analytical grade and were used as received. Tetra-*n*-butylammonium hexafluorophosphate (Aldrich, 98 %) was recrystallized for no less than three times from hot absolute ethanol prior to use. All reactions were performed under anaerobic and anhydrous conditions using standard Schlenk techniques under an inert atmosphere of nitrogen.

Physical measurements and instrumentation. ^{1}H, ^{13}C{^{1}H} and ^{31}P{^{1}H} NMR spectra were recorded on a Bruker Avance 500 (500 MHz for ^{1}H; 125 MHz for ^{13}C{^{1}H} nuclei; 202 MHz for ^{31}P{^{1}H}) or 600 (150 MHz for ^{13}C{^{1}H} nuclei) Fourier-transform NMR spectrometer with chemical shifts reported relative to tetramethylsilane, with the residual NMR solvent peak used as internal reference (δ 7.26 ppm for chloroform, δ 1.72 or δ 3.58 ppm for tetrahydrofuran). Splitting of the ^{13}C signal due to ^{31}P–^{13}C coupling was not determined; instead, all of them were reported as individual singlet peaks. High Resolution ESI mass spectra were recorded on Bruker maXis II^{TM} High Resolution LC-QTOF Mass Spectrometer. IR spectra were recorded on a PerkinElmer Spectrum Two FT-IR spectrometer (8300−350 cm^{-1}). The UV-vis absorption spectra were recorded on a Cary 60 UV-vis (Agilent Technology) spectrophotometer equipped with a Xenon flash lamp. Samples for photophysical measurements were degassed with no less than four freeze−pump−thaw cycles on the high-vacuum line prior to measurements. Steady-state excitation and emission spectra were recorded on a Horiba Scientific FluoroMax-4 fluorescence spectrofluorometer equipped with a R928P PMT detector. Liquid nitrogen was placed into the quartz-walled optical Dewar flask for low-temperature (77 K) photophysical measurements. Transient absorption measurements were performed on a LP920 laser flash photolysis spectrometer (Edinburgh Instruments Ltd., Livingston U.K.) at ambient temperature. The excitation source was the 355-nm output (third harmonic of a Nd:YAG laser (Spectra-Physics Quanta-Ray Lab130 Pulsed Nd:YAG Laser), and the probe light source was a Xe900 450W xenon arc lamp. The transient absorption spectra were detected by an image intensified CCD camera (Andor) with PC plug-in controller, fully operated by L900 spectrometer software. The absorption kinetics were detected by a Hamamatsu R928 photomultiplier tube and recorded on a Tektronix model TDS3012B (100MHz, 1.25 GS/s) digital oscilloscope and analyzed using the same software for exponential fit. Solid-state photophysical measurements were performed with

solid sample loaded into a quartz tube inside a quartz-walled Dewar flask. Excited-state lifetimes of solution, solid and glass samples were measured with an Edinburgh Instruments LP980 Spectrometer. The excitation source used was the 355 nm output (third harmonic, 8 ns) of a Spectra-Physics Quanta-Ray Q-switched GCR-150 pulsed Nd:YAG laser (10 Hz). Luminescence decay signals were recorded by a Hamamatsu R928 photomultiplier tube, recorded on a Tektronix model TDS-620A (500 MHz, 2 GSs^{-1}) digital oscilloscope, and analyzed with a program for exponential fits. Relative photoluminescence quantum yields in solution were measured by the optical dilute method reported by Demas and Crosby.[8] A degassed solution of quinine sulphate in 1N H_2SO_4 has been used as reference (Φ_{lum} = 0.546, excitation wavelength at 365 nm),[8] whereas absolute photoluminescence quantum yields (PLQYs) in thin films were measured on a Hamamatsu C11347-11 Quantaurus-QY Absolute PL Quantum Yield Spectrometer. Excited-state lifetimes of thin films were measured on a Quantaurus-Tau C11367−34 fluorescence lifetime spectrometer. Cyclic voltammetry was performed with a CH Instruments Model CHI620E (CH Instruments, Inc.). All solutions for electrochemical measurements were purged with prepurified argon gas prior to measurement. Thermal analyses were performed on a TGA Q50 (TA Instruments), PerkinElmer STA 6000 Simultaneous Thermal Analyzer and NETZSCH TG209 system, in which T_d is defined as the extrapolated onset temperature of the TGA curve.

Synthesis. 3-Cyano-9*H*-carbazole,[9] 3-(diphenylphosphoryl)-9*H*-carbazole[10] and the 4-(diphenylamino)aryl-substituted carbazolyl ligands[11] (i.e. 4-(9*H*-carbazol-3-yl)-*N*,*N*-diphenylamine, 4-(9*H*-carbazol-3-yl)-3-methyl-*N*,*N*-diphenylamine, 4-(9*H*-carbazol-2-yl)-*N*,*N*-diphenylamine and 4-(9*H*-carbazol-2-yl)-3-methyl-*N*,*N*-diphenylamine) were prepared according to the literature procedures. The chlorogold(III) precursor complex, [Au{4-^{t}BuC^C(4-^{t}BuC_6H_4)^N}Cl], was prepared by a method according to the reported literature procedure previously reported by us.[12] The carbazolylgold(III) complexes were then synthesized by reacting the corresponding carbazolyl ligands with the chlorogold(III) complex with sodium hydride in degassed tetrahydrofuran.[12]

[Au{4-^{t}BuC^C(4-^{t}BuC_6H_4)^N}(3-CN-Cbz)] (**1**). A mixture of [Au{4-^{t}BuC^C(4-^{t}BuC_6H_4)^N}Cl] (50 mg, 0.08 mmol), NaH (3 mg, 0.12 mmol) and 3-cyano-9*H*-carbazole (16 mg, 0.08 mmol) in degassed tetrahydrofuran solution (15 ml) was stirred overnight at room temperature. After removing the solvent, the crude product was filtered and washed

with minimal amount of diethyl ether. Subsequent recrystallization by diffusion of diethyl ether vapor into a concentrated dichloromethane solution of product gave **1** as a pale yellow solid. Yield: 35 mg, 55 %. ^{1}H NMR (500 MHz, $CDCl_3$, 298 K, relative to Me_4Si, δ/ppm): δ 8.54 (d, J = 1.5 Hz, 1H, carbazolyl proton), 8.26−8.24 (d, J = 7.9 Hz, 1H, carbazolyl proton), 8.05−7.99 (m, 3H, pyridyl protons of 4-^{t}BuC^C(4-^{t}BuC_6H_4)^N), 7.70−7.68 (d, J = 7.9 Hz, 1H, carbazolyl proton), 7.64−7.61 (m, 4H, carbazolyl proton and phenyl protons of 4-^{t}BuC^C(4-^{t}BuC_6H_4)^N), 7.59 (d, J = 1.5 Hz, 1H, phenyl proton of 4-^{t}BuC^C(4-^{t}BuC_6H_4)^N), 7.56−7.54 (d, J = 8.4 Hz, 2H, phenyl protons of 4-^{t}BuC^C(4-^{t}BuC_6H_4)^N), 7.53−7.51 (dd, J = 8.5 and 1.5 Hz, 1H, carbazolyl proton), 7.40−7.35 (m, 2H, carbazolyl proton and phenyl proton of 4-^{t}BuC^C(4-^{t}BuC_6H_4)^N), 7.25−7.22 (m, 2H, carbazolyl proton and pyridyl proton of 4-^{t}BuC^C(4-^{t}BuC_6H_4)^N), 7.19−7.17 (dd, J = 8.0 and 1.9 Hz, 1H, phenyl proton of 4-^{t}BuC^C(4-^{t}BuC_6H_4)^N), 6.67 (d, J = 1.9 Hz, 1H, phenyl proton of 4-^{t}BuC^C(4-^{t}BuC_6H_4)^N), 1.41 (s, 9H, −^{t}Bu), 0.91 (s, 9H, −^{t}Bu). ^{13}C{^{1}H} NMR (125 MHz, $CDCl_3$, 298 K, relative to Me_4Si, δ/ppm): δ 164.73, 164.54, 151.83, 151.74, 151.44, 151.17, 150.13, 149.54, 148.97, 147.97, 142.50, 141.45, 141.28, 138.16, 131.62, 127.21, 126.94, 125.97, 125.57, 125.37, 125.29, 125.13, 124.56, 124.54, 122.35, 122.14, 121.98, 120.55, 120.45, 120.40, 118.15, 114.24, 114.04, 98.04, 34.74, 34.68, 31.39, 30.76. HRMS (Positive ESI): Found m/z 806.2799 $[M+H]^+$. Calcd for $AuC_{44}H_{39}N_3$: m/z 806.2804. Elemental analyses: Found (%): C 65.37, H 4.71, N 5.25. Calcd for $AuC_{44}H_{38}N_3$: C 65.59, H 4.75, N 5.21. IR 2213 cm^{-1} ν(C≡N).

[Au{4-^{t}BuC^C(4-^{t}BuC_6H_4)^N}(3-(P(O)Ph_2)-Cbz)] (**2**). This complex was synthesized with the same procedure as **1** except that 3-cyano-9*H*-carbazole was replaced by 3-(diphenylphosphoryl)-9*H*-carbazole (113 mg, 0.31 mmol). Pale yellow solid. Yield: 142 mg, 47 %. ^{1}H NMR (500 MHz, $CDCl_3$, 298 K, relative to Me_4Si, δ/ppm): δ 8.60−8.57 (dd, J = 12.8 and 1.2 Hz, 1H, carbazolyl proton), 8.19−8.17 (d, J = 7.8 Hz, 1H, carbazolyl proton), 8.09−8.08 (d, J = 5.1 Hz, 1H, pyridyl proton of 4-^{t}BuC^C(4-^{t}BuC_6H_4)^N), 8.03−7.97 (m, 2H, pyridyl protons of 4-^{t}BuC^C(4-^{t}BuC_6H_4)^N), 7.78−7.74 (m, 4H, −C_6H_5 of phosphine oxide), 7.68−7.65 (m, 2H, carbazolyl protons), 7.62−7.61 (d, J = 8.4 Hz, 2H, phenyl protons of 4-^{t}BuC^C(4-^{t}BuC_6H_4)^N), 7.60 (d, J = 1.2 Hz, 1H, phenyl proton of 4-^{t}BuC^C(4-^{t}BuC_6H_4)^N), 7.58−7.57 (d, J = 1.2 Hz, 1H, phenyl proton of 4-^{t}BuC^C(4-^{t}BuC_6H_4)^N), 7.55−7.42 (m, 9H,

$-C_6H_5$ of phosphine oxide, carbazolyl proton and phenyl protons of 4-^{t}BuC^C(4-^{t}BuC_6H_4)^N), 7.36−7.32 (m, 2H, carbazolyl proton and phenyl proton of 4-^{t}BuC^C(4-^{t}BuC_6H_4)^N), 7.25−7.23 (m, 1H, pyridyl proton of 4-^{t}BuC^C(4-^{t}BuC_6H_4)^N), 7.18−7.14 (m, 2H, carbazolyl proton and phenyl proton of 4-^{t}BuC^C(4-^{t}BuC_6H_4)^N), 6.74−6.73 (d, J = 1.9 Hz, 1H, phenyl proton of 4-^{t}BuC^C(4-^{t}BuC_6H_4)^N), 1.40 (s, 9H, $-^t$Bu), 0.92 (s, 9H, $-^t$Bu). $^{13}C\{^1H\}$ NMR (125 MHz, tetrahydofuran-d_8, 298 K, δ/ppm): δ 165.40, 165.26, 152.94, 152.19, 151.25, 150.99, 150.97, 150.42, 149.77, 148.75, 143.00, 142.82, 142.64, 139.03, 137.15, 137.07, 136.34, 136.26, 132.84, 132.81, 132.77, 132.73, 132.18, 131.51, 131.49, 131.46, 131.44, 128.67, 128.65, 128.58, 128.55, 127.89, 127.80, 127.50, 126.27, 126.02, 125.88, 125.75, 125.35, 125.26, 122.48, 122.28, 121.72, 121.21, 120.69, 119.84, 118.95, 117.88, 114.53, 114.20, 114.10, 35.11, 35.02, 31.50, 31.02. $^{31}P\{^1H\}$ NMR (202 MHz, $CDCl_3$, 298 K, relative to Me_4Si, δ/ppm): δ 31.68. HRMS (Positive ESI): Found m/z 980.3146 $[M+H]^+$. Calcd for $AuC_{55}H_{49}N_2OP$: m/z 980.3164. Elemental analyses: Found (%): C 66.18, H 4.91, N 2.72. Calcd for $AuC_{55}H_{48}N_2OP{\cdot}H_2O$: C 66.13, H 5.05, N 2.80. IR 1102 cm^{-1} ν(P=O).

[Au{4-^{t}BuC^C(4-^{t}BuC_6H_4)^N}(3-(C_6H_4-NPh_2)-Cbz)] (**3**). This complex was synthesized with the same procedure as **1** except that 3-cyano-9*H*-carbazole was replaced by 4-(9*H*-carbazol-3-yl)-*N*,*N*-diphenylaniline (32 mg, 0.08 mmol). Orange solid. Yield: 38 mg, 48 %. ^1H NMR (500 MHz, $CDCl_3$, 298 K, relative to Me_4Si, δ/ppm): δ 8.45 (d, J = 1.7 Hz, 1H, carbazolyl proton), 8.29−8.27 (d, J = 7.7 Hz, 1H, carbazolyl proton), 8.15−8.14 (d, J = 5.4 Hz, 1H, pyridyl proton of 4-^{t}BuC^C(4-^{t}BuC_6H_4)^N), 8.02−7.97 (m, 2H, pyridyl protons of 4-^{t}BuC^C(4-^{t}BuC_6H_4)^N), 7.67−7.62 (m, 6H, $-C_6H_4-$ of triphenylamine, carbazolyl protons and phenyl protons of 4-^{t}BuC^C(4-^{t}BuC_6H_4)^N), 7.61 (d, J = 1.2 Hz, 1H, phenyl proton of 4-^{t}BuC^C(4-^{t}BuC_6H_4)^N), 7.59 (d, J = 1.2 Hz, 1H, phenyl proton of 4-^{t}BuC^C(4-^{t}BuC_6H_4)^N), 7.56−7.54 (m, 3H, carbazolyl proton and phenyl protons of 4-^{t}BuC^C(4-^{t}BuC_6H_4)^N), 7.37−7.35 (d, J = 8.0 Hz, 1H, phenyl proton of 4-^{t}BuC^C(4-^{t}BuC_6H_4)^N), 7.32−7.29 (t, J = 7.7 Hz, 1H, carbazolyl proton), 7.28−7.25 (m, 4H, $-C_6H_5$ of triphenylamine), 7.23−7.21 (m, 1H, pyridyl proton of 4-^{t}BuC^C(4-^{t}BuC_6H_4)^N), 7.19−7.12 (m, 8H, $-C_6H_4-$ of triphenylamine, $-C_6H_5$ of triphenylamine, carbazolyl proton and phenyl proton of 4-

^{t}BuC^C(4-^{t}BuC$_6$H$_4$)^N), 7.02−6.99 (t, J = 7.3 Hz, 2H, −C$_6$H$_5$ of triphenylamine), 6.85 (d, J = 1.9 Hz, 1H, phenyl proton of 4-^{t}BuC^C(4-^{t}BuC$_6$H$_4$)^N), 1.41 (s, 9H, −^{t}Bu), 0.93 (s, 9H, −^{t}Bu). ^{13}C{^{1}H} NMR (125 MHz, CDCl$_3$, 298 K, relative to Me$_4$Si, δ/ppm): δ 165.36, 164.94, 152.00, 151.81, 151.67, 151.15, 150.05, 148.98, 148.16, 148.13, 147.85, 145.77, 142.32, 141.56, 141.33, 138.51, 138.05, 132.28, 129.31, 127.92, 127.09, 126.07, 125.93, 125.66, 124.98, 124.49, 124.36, 124.33, 124.09, 123.52, 122.54, 122.29, 121.88, 120.49, 120.45, 120.18, 118.27, 116.63, 113.94, 113.92, 34.90, 34.81, 31.54, 30.96. HRMS (Positive ESI): Found m/z 1024.3902 [M+H]$^+$. Calcd for AuC$_{61}$H$_{53}$N$_3$: m/z 1024.3900. Elemental analyses: Found (%): C 69.62, H 5.21, N 3.74. Calcd for AuC$_{61}$H$_{52}$N$_3$·1.5H$_2$O: C 69.71, H 5.27, N 4.00.

[Au{4-^{t}BuC^C(4-^{t}BuC$_6$H$_4$)^N}(3-(MeC$_6$H$_3$-NPh$_2$)-Cbz)] (**4**). This complex was synthesized with the same procedure as **1** except that 3-cyano-9*H*-carbazole was replaced by 4-(9*H*-carbazol-3-yl)-3-methyl-*N*,*N*-diphenylaniline (33 mg, 0.08 mmol). Yellowish orange solid. Yield: 52 mg, 65 %. ^{1}H NMR (500 MHz, CDCl$_3$, 298 K, relative to Me$_4$Si, δ/ppm): δ 8.26−8.23 (m, 2H, carbazolyl proton and pyridyl proton of 4-^{t}BuC^C(4-^{t}BuC$_6$H$_4$)^N), 8.20 (d, J = 1.4 Hz, 1H, carbazolyl proton), 8.03−7.98 (m, 2H, pyridyl protons of 4-^{t}BuC^C(4-^{t}BuC$_6$H$_4$)^N), 7.66−7.62 (m, 4H, carbazolyl protons and phenyl protons of 4-^{t}BuC^C(4-^{t}BuC$_6$H$_4$)^N), 7.62−7.61 (d, J = 1.3 Hz, 1H, phenyl proton of 4-^{t}BuC^C(4-^{t}BuC$_6$H$_4$)^N), 7.59 (d, J = 1.3 Hz, 1H, phenyl proton of 4-^{t}BuC^C(4-^{t}BuC$_6$H$_4$)^N), 7.56−7.54 (d, J = 8.4 Hz, 2H, phenyl protons of 4-^{t}BuC^C(4-^{t}BuC$_6$H$_4$)^N), 7.36−7.35 (d, J = 8.0 Hz, 1H, phenyl proton of 4-^{t}BuC^C(4-^{t}BuC$_6$H$_4$)^N), 7.30−7.23 (m, 8H, carbazolyl protons, phenyl proton of −MeC$_6$H$_3$−, −C$_6$H$_5$ of diphenylamine and pyridyl proton of 4-^{t}BuC^C(4-^{t}BuC$_6$H$_4$)^N), 7.18−7.16 (m, 5H, −C$_6$H$_5$ of diphenylamine and phenyl proton of 4-^{t}BuC^C(4-^{t}BuC$_6$H$_4$)^N), 7.14−7.11 (t, J = 7.3 Hz, 1H, carbazolyl proton), 7.05 (d, J = 2.1 Hz, 1H, phenyl proton of −MeC$_6$H$_3$−), 7.02–6.98 (m, 3H, phenyl proton of −MeC$_6$H$_3$−, −C$_6$H$_5$ of diphenylamine), 6.81−6.80 (d, J = 1.9 Hz, 1H, phenyl proton of 4-^{t}BuC^C(4-^{t}BuC$_6$H$_4$)^N), 2.30 (s, 3H, −Me), 1.41 (s, 9H, −^{t}Bu), 0.93 (s, 9H, −^{t}Bu). ^{13}C{^{1}H} NMR (150 MHz, CDCl$_3$, 298 K, relative to Me$_4$Si, δ/ppm): δ 165.43, 164.97, 152.02, 151.71, 151.66, 151.13, 150.14, 148.92, 148.25, 148.10, 147.33, 145.95, 142.28, 141.56, 141.35, 138.94, 138.51, 136.90, 132.29, 131.44, 130.00, 129.27, 127.09, 126.27, 126.07, 125.91, 125.55, 125.27, 124.96, 124.45, 124.29,

124.22, 124.10, 122.40, 122.29, 122.11, 121.85, 120.73, 120.48, 120.45, 120.15, 116.46, 113.63, 113.41, 34.90, 34.80, 31.54, 30.95, 21.16. HRMS (Positive ESI): Found *m/z* 1038.4045 $[M+H]^+$. Calcd for $AuC_{62}H_{55}N_3$: *m/z* 1038.4056. Elemental analyses: Found (%): C 71.43, H 5.43, N 4.06. Calcd for $AuC_{62}H_{54}N_3$: C 71.74, H 5.24, N 4.05.

[Au{4-^{t}BuC^C(4-^{t}BuC_6H_4)^N}(2-(C_6H_4-NPh_2)-Cbz)] (**5**). This complex was synthesized with the same procedure as **1** except that 3-cyano-9*H*-carbazole was replaced by 4-(9*H*-carbazol-2-yl)-*N*,*N*-diphenylaniline (32 mg, 0.08 mmol). Yellow solid. Yield: 41 mg, 52 %. ^{1}H NMR (500 MHz, $CDCl_3$, 298 K, relative to Me_4Si, δ/ppm): δ 8.28−8.26 (d, *J* = 8.1 Hz, 1H, carbazolyl proton), 8.26−8.24 (d, *J* = 7.6 Hz, 1H, carbazolyl proton), 8.18−8.17 (d, *J* = 5.3 Hz, 1H, pyridyl proton of 4-^{t}BuC^C(4-^{t}BuC_6H_4)^N), 8.01−7.97 (m, 2H, pyridyl protons of 4-^{t}BuC^C(4-^{t}BuC_6H_4)^N), 7.81−7.80 (d, *J* = 1.2 Hz, 1H, carbazolyl proton), 7.64−7.61 (m, 3H, carbazolyl proton and phenyl protons of 4-^{t}BuC^C(4-^{t}BuC_6H_4)^N), 7.60 (d, *J* = 1.4 Hz, 1H, phenyl proton of 4-^{t}BuC^C(4-^{t}BuC_6H_4)^N), 7.58 (d, *J* = 1.4 Hz, 1H, phenyl proton of 4-^{t}BuC^C(4-^{t}BuC_6H_4)^N), 7.56−7.54 (d, *J* = 8.4 Hz, 2H, phenyl protons of 4-^{t}BuC^C(4-^{t}BuC_6H_4)^N), 7.48−7.46 (d, *J* = 8.7 Hz, 2H, −C_6H_4− of triphenylamine), 7.38−7.34 (m, 2H, carbazolyl proton and phenyl proton of 4-^{t}BuC^C(4-^{t}BuC_6H_4)^N), 7.31−7.28 (td, *J* = 7.6 and 1.2 Hz, 1H, carbazolyl proton), 7.23−7.20 (m, 5H, pyridyl proton of 4-^{t}BuC^C(4-^{t}BuC_6H_4)^N and −C_6H_5 of triphenylamine), 7.17−7.15 (dd, *J* = 8.0 and 2.0 Hz, 1H, phenyl proton of 4-^{t}BuC^C(4-^{t}BuC_6H_4)^N), 7.15−7.12 (m, 1H, carbazolyl proton), 7.09−7.07 (d, *J* = 7.4 Hz, 4H, −C_6H_5 of triphenylamine), 7.06−7.04 (d, *J* = 8.7 Hz, 2H, −C_6H_4− of triphenylamine), 6.98−6.95 (t, *J* = 7.4 Hz, 2H, −C_6H_5 of triphenylamine), 6.86−6.85 (d, *J* = 2.0 Hz, 1H, phenyl proton of 4-^{t}BuC^C(4-^{t}BuC_6H_4)^N), 1.40 (s, 9H, −^{t}Bu), 0.90 (s, 9H, −^{t}Bu). $^{13}C\{^1H\}$ NMR (150 MHz, $CDCl_3$, 298 K, relative to Me_4Si, δ/ppm): δ 165.44, 164.97, 151.98, 151.76, 151.67, 151.12, 150.03, 149.02, 148.95, 148.13, 147.99, 146.29, 142.32, 141.57, 141.35, 138.54, 137.76, 137.08, 132.23, 129.27, 128.34, 127.09, 126.07, 125.28, 125.01, 124.54, 124.48, 124.46, 124.17, 122.62, 122.29, 121.86, 120.49, 120.48, 120.29, 120.13, 116.57, 116.04, 113.65, 111.93, 34.87, 34.81, 31.54, 30.94. HRMS (Positive ESI): Found *m/z* 1024.3909 $[M+H]^+$. Calcd for $AuC_{61}H_{53}N_3$: *m/z* 1024.3900. Elemental analyses: Found (%): C 71.27, H 5.36, N 3.98. Calcd for $AuC_{61}H_{52}N_3$: C 71.54, H 5.12, N 4.10.

[Au{4-^{t}BuC^C(4-^{t}BuC_6H_4)^N}(2-(MeC_6H_3-NPh_2)-Cbz)] (**6**). This complex was synthesized with the same procedure as **1** except that 3-cyano-9*H*-carbazole was replaced by 4-(9*H*-carbazol-2-yl)-3-methyl-*N*,*N*-diphenylaniline (64 mg, 0.15 mmol). Yellow solid. Yield: 83 mg, 52 %. ^{1}H NMR (500 MHz, $CDCl_3$, 298 K, relative to Me_4Si, δ/ppm): δ 8.26−8.24 (m, 2H, carbazolyl protons), 8.15−8.14 (d, J = 5.2 Hz, 1H, pyridyl proton of 4-^{t}BuC^C(4-^{t}BuC_6H_4)^N), 8.00−7.95 (m, 2H, pyridyl protons of 4-^{t}BuC^C(4-^{t}BuC_6H_4)^N), 7.65−7.63 (d, J = 8.1 Hz, 1H, carbazolyl proton), 7.62−7.60 (d, J = 8.3 Hz, 2H, phenyl protons of 4-^{t}BuC^C(4-^{t}BuC_6H_4)^N), 7.59−7.57 (m, 3H, carbazolyl proton and phenyl protons of 4-^{t}BuC^C(4-^{t}BuC_6H_4)^N), 7.55−7.53 (d, J = 8.3 Hz, 2H, phenyl protons of 4-^{t}BuC^C(4-^{t}BuC_6H_4)^N), 7.35−7.33 (d, J = 8.0 Hz, 1H, phenyl proton of 4-^{t}BuC^C(4-^{t}BuC_6H_4)^N), 7.32−7.28 (td, J = 8.1 and 1.2 Hz, 1H, carbazolyl proton), 7.22−7.19 (m, 5H, −C_6H_5 of diphenylamine and pyridyl proton of 4-^{t}BuC^C(4-^{t}BuC_6H_4)^N), 7.17−7.11 (m, 4H, carbazolyl protons, phenyl proton of 4-^{t}BuC^C(4-^{t}BuC_6H_4)^N and phenyl proton of −MeC_6H_3−), 7.09−7.07 (d, J = 7.5 Hz, 4H, − C_6H_5 of diphenylamine), 6.97−6.94 (t, J = 7.5 Hz, 2H, − C_6H_5 of diphenylamine), 6.92−6.91 (d, J = 2.2 Hz, 1H, phenyl proton of −MeC_6H_3−), 6.86−6.84 (dd, J = 8.3 and 2.2 Hz, 1H, phenyl proton of −MeC_6H_3−), 6.83 (d, J = 2.0 Hz, 1H, phenyl proton of 4-^{t}BuC^C(4-^{t}BuC_6H_4)^N, 2.14 (s, 3H, −Me), 1.40 (s, 9H, −^{t}Bu), 0.92 (s, 9H, −^{t}Bu). ^{13}C{^{1}H} NMR (125 MHz, $CDCl_3$, 298 K, relative to Me_4Si, δ/ppm): δ 165.42, 164.95, 151.99, 151.75, 151.65, 151.12, 150.02, 148.86, 148.44, 148.16, 148.14, 146.15, 142.30, 141.54, 141.31, 138.72, 138.52, 137.80, 136.60, 132.11, 131.21, 129.22, 127.09, 126.06, 126.03, 125.29, 125.06, 124.41, 124.12, 124.02, 122.42, 122.27, 121.85, 121.79, 120.47, 120.44, 120.08, 119.39, 118.43, 116.50, 114.35, 113.60, 34.88, 34.80, 31.54, 31.00, 21.14. HRMS (Positive ESI): Found *m*/*z* 1038.4073 $[M+H]^+$. Calcd for $AuC_{62}H_{55}N_3$: *m/z* 1038.4056. Elemental analyses: Found (%): C 71.43, H 5.26, N 4.06. Calcd for $AuC_{62}H_{54}N_3$: C 71.74, H 5.24, N 4.05.

Molecular orientation measurements.

The gold(III) complexes doped in 3,3′-di(9*H*-carbazol-9-yl)-1,1′-biphenyl (*m*-CBP) thin films were prepared by thermal evaporation on top of precleaned bare silicon substrates. The refractive index and thickness of the films were then determined by the alpha-SE

Ellipsometer (J. A. Woollam). Then, 20-nm thick thin films were fabricated on glass substrates that were carefully pre-washed in the same manner as the fused silica substrates. The dipole orientation of the gold(III) complexes was estimated by the Molecular Orientation Characteristic Measurement System (C14234-11, Hamamatsu Photonics). All the thin films were freshly prepared to avoid photodegradation of the materials during the measurement. The samples were then attached to a cylindrical lens, with the refractive index of 1.5, via matching oil, and mounted on an automated rotational stage with the film surface precisely positioned at the rotational center of the stage. Photoexcitation of the samples (λ = 365 nm, Power = ~1.5 mW) was performed using a fiber-guided LED output source. The emission from the sample was then collected by a Photonic Multi-Channel Analyzer PMA-12 (C10027-01, Hamamatsu Photonics) through a long-pass filter and a transverse magnetic (TM) mode polarizer. The estimated p_z and order parameter (S) were calculated by the Standard Software (U6039-09, Hamamatsu Photonics), and the angle θ between the normal of a substrate and transition dipole was then calculated by the equation, $S = \frac{1}{2}\langle 3\cos^2\theta - 1\rangle$, with the bracketed values indicating an ensemble average of $\langle\cos^2\theta\rangle$.[2] The ratio of the horizontal dipoles to the total dipoles of the emitters (Θ) isobtained by the equation Θ:(1 − Θ) =$\langle\sin^2\theta\rangle$:$\langle\cos^2\theta\rangle$ = h:v.[3]

Computational details.

All ground state molecules (S_0) were optimized at density functional theory (DFT) level of theory with the PBE0 hybrid functional[13-15] and 6-31G(d,p) basis set.[16-18] The excited state geometries were optimized at time-dependent density functional theory (TD-DFT)[19-21] level of theory. Geometry optimizations were calculated in an implicit solvent environment (toluene) described by the conductor-like polarizable continuum model (CPCM)[22,23] and with a pruned (175,974) grid for numerical integration. Grimme's dispersion with the D3 damping function (GD3) were included for atom-pairwise dispersion corrections. Stuttgart effective core potentials (ECPs) and the associated basis set were used to describe the Au atom[24] with additional f-type polarization functions.[25] All the calculations described above were carried out with the Gaussian 16 suite of program.[26] The Cartesian coordinates of the optimized S_0, S_1 and T_1 geometries of **1**, **2** and **6** are given in **Tables S4**–**S10**. The photophysical data and SOC matrix elements for all the excited state molecules were calculated using TD-DFT method with the PBE0 hybrid functional and Slater-type all-electron basis set (TZV) using the ADF2019 package. Scalar and spin-orbit relativistic effects were employed to describe

the excited state S_1 and T_1 respectively by using zeroth-order regular approximation (ZORA) formalism in ADF package. The SOC matrix element, $\langle S_1|\hat{H}_{SO}|T_1\rangle$, is calculated by averaging the three degenerate T_1 substates (m=0, ±1). COSMO continuum solvation model was used to describe the solvation effect.

OLED fabrication and measurements. OLEDs were fabricated on patterned ITO glass substrates. The substrates were cleaned with Decon 90, rinsed with deionized water then dried in an oven, and finally treated in an ultraviolet-ozone chamber. In particular, a 40-nm thick PEDOT:PSS was spin-coated onto the ITO coated glass substrates as hole-transporting layer. After that, the emissive layer was formed by mixing gold(III) complex with MCP to prepare a 10 mg cm^{-3} solution in chloroform and spin-coating onto PEDOT:PSS layer to give uniform thin films of 30-nm thickness. Onto this, a 5-nm thick 3TPyMB and a 40-nm thick TmPyPB were evaporated as a hole-blocking layer and an electron-transporting layer, respectively; while a LiF/Al was used as the metal cathode. All films were sequentially deposited at a rate of 0.1−0.2 nm s^{-1} without vacuum break. A shadow mask was used to define the cathode and to make four 0.1 cm^2 devices on each substrate. Current density–voltage–luminance characteristics and electroluminescence spectra were measured simultaneously with a programmable Keithley model 2420 power source and a Photoresearch PR-655 spectrometer.

^{1}H NMR spectra of gold(III) complexes.

[Au{4-^{t}BuC^C(4-^{t}BuC$_6$H$_4$)^N}(3-CN-Cbz)] (**1**)

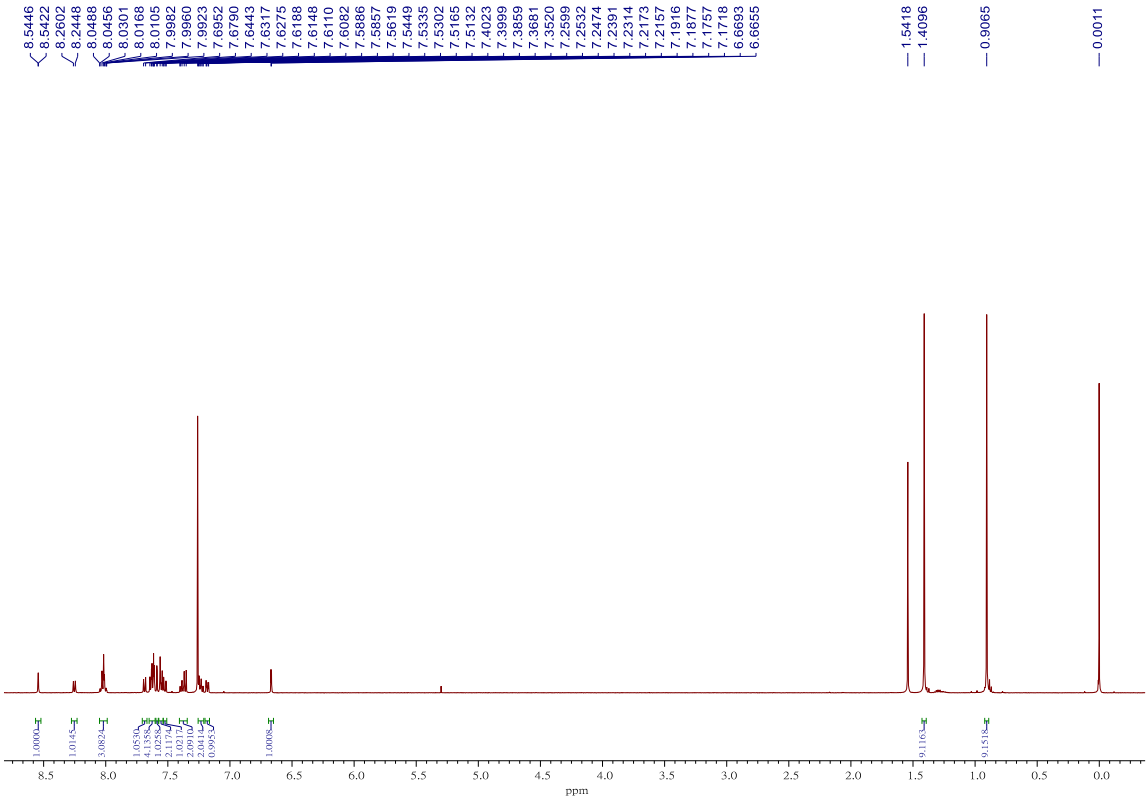

[Au{4-^{t}BuC^C(4-^{t}BuC$_6$H$_4$)^N}(3-(P(O)Ph$_2$)-Cbz)] (**2**)

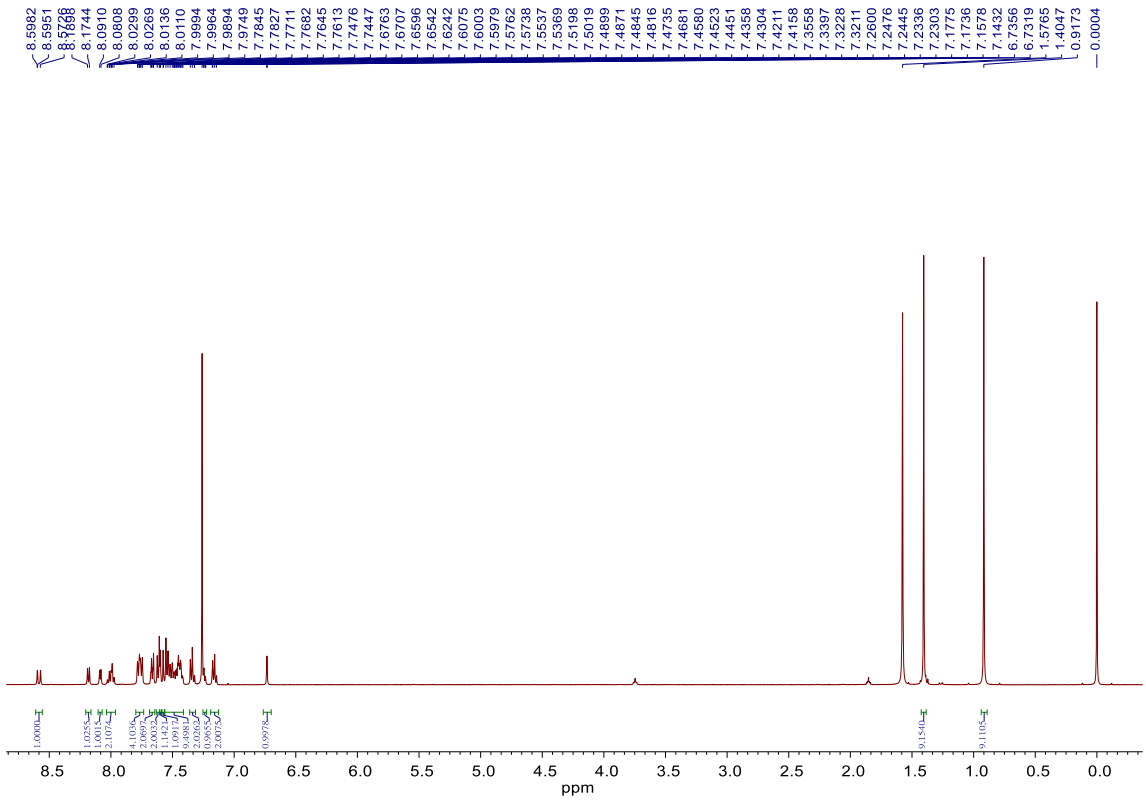

[Au{4-^{t}BuC^C(4-^{t}BuC_6H_4)^N}(3-(C_6H_4-NPh_2)-Cbz)] (**3**)

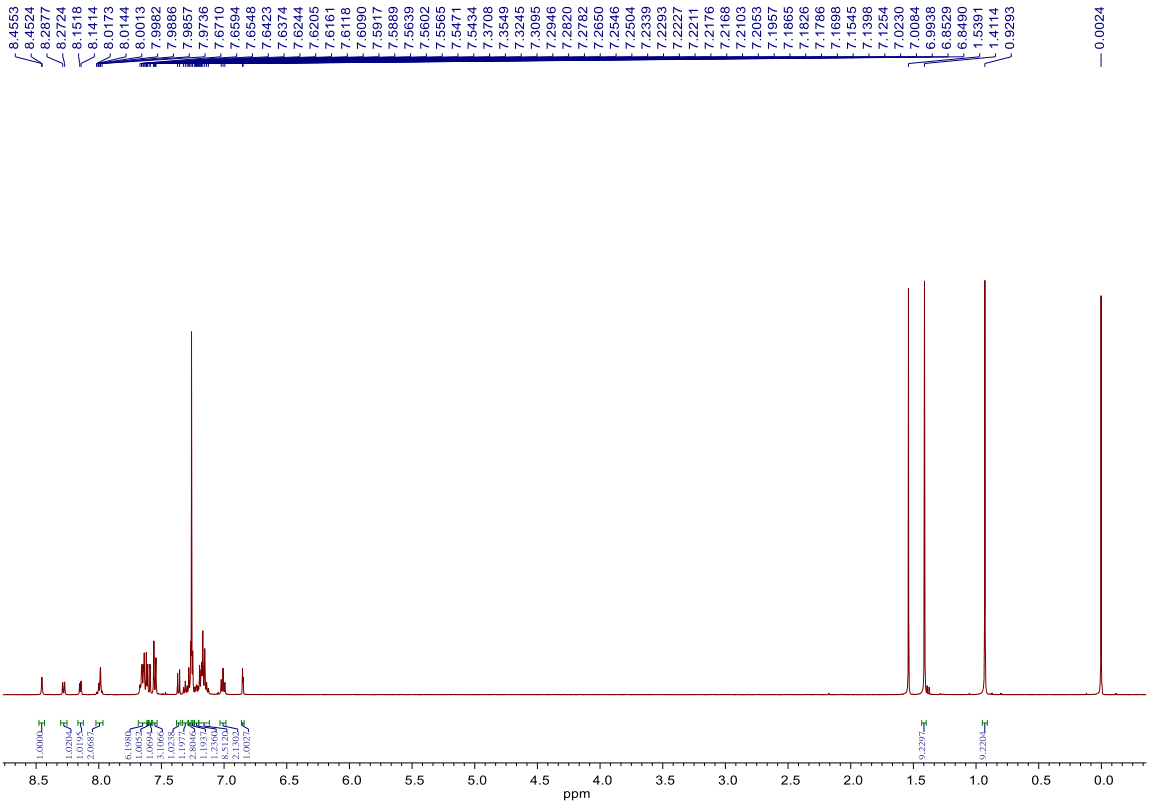

[Au{4-^{t}BuC^C(4-^{t}BuC_6H_4)^N}(3-(MeC_6H_3-NPh_2)-Cbz)] (**4**)

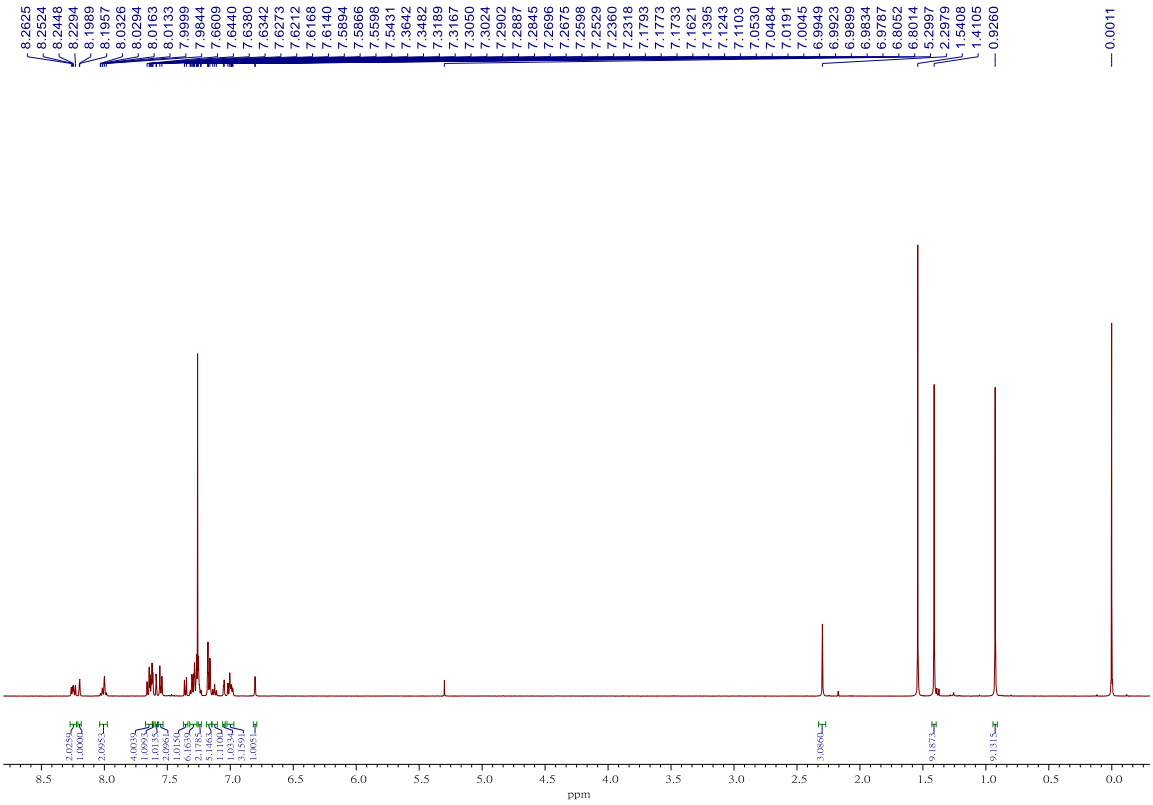

[Au{4-^{t}BuC^C(4-^{t}BuC_6H_4)^N}(2-(C_6H_4-NPh_2)-Cbz)] (**5**)

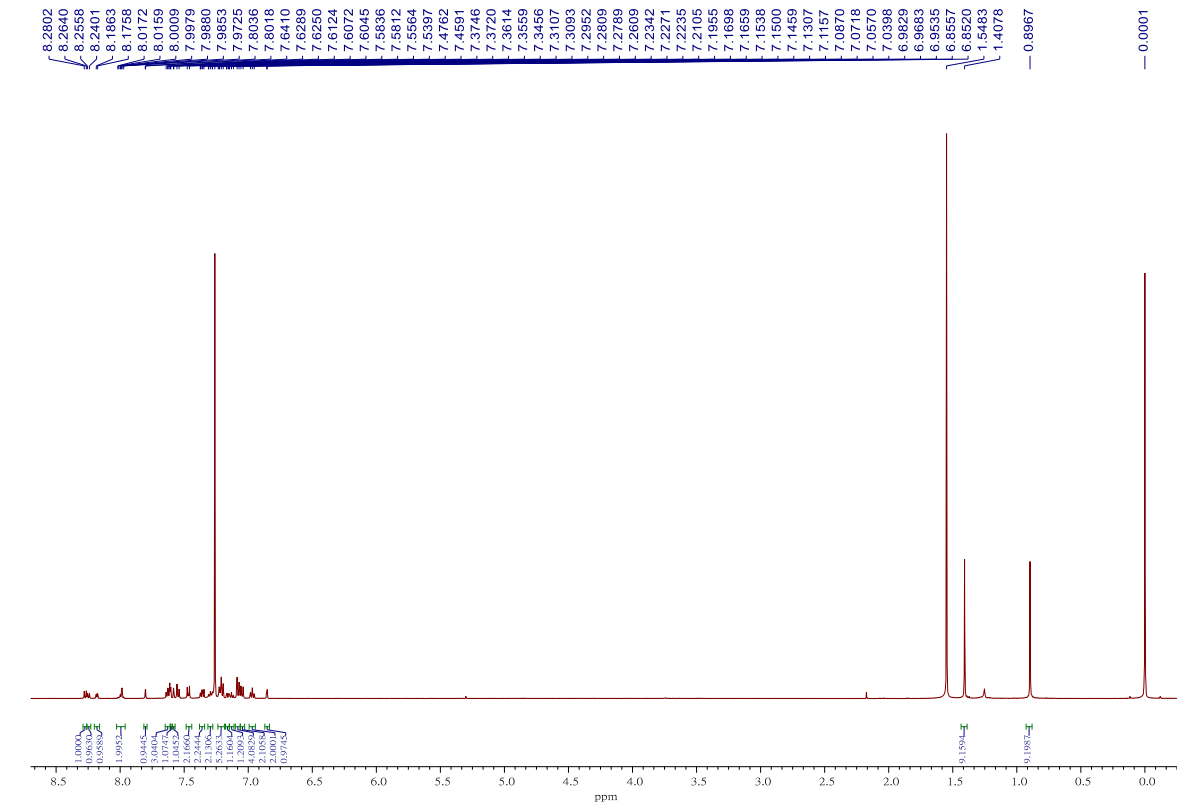

[Au{4-^{t}BuC^C(4-^{t}BuC_6H_4)^N}(2-(MeC_6H_3-NPh_2)-Cbz)] (**6**)

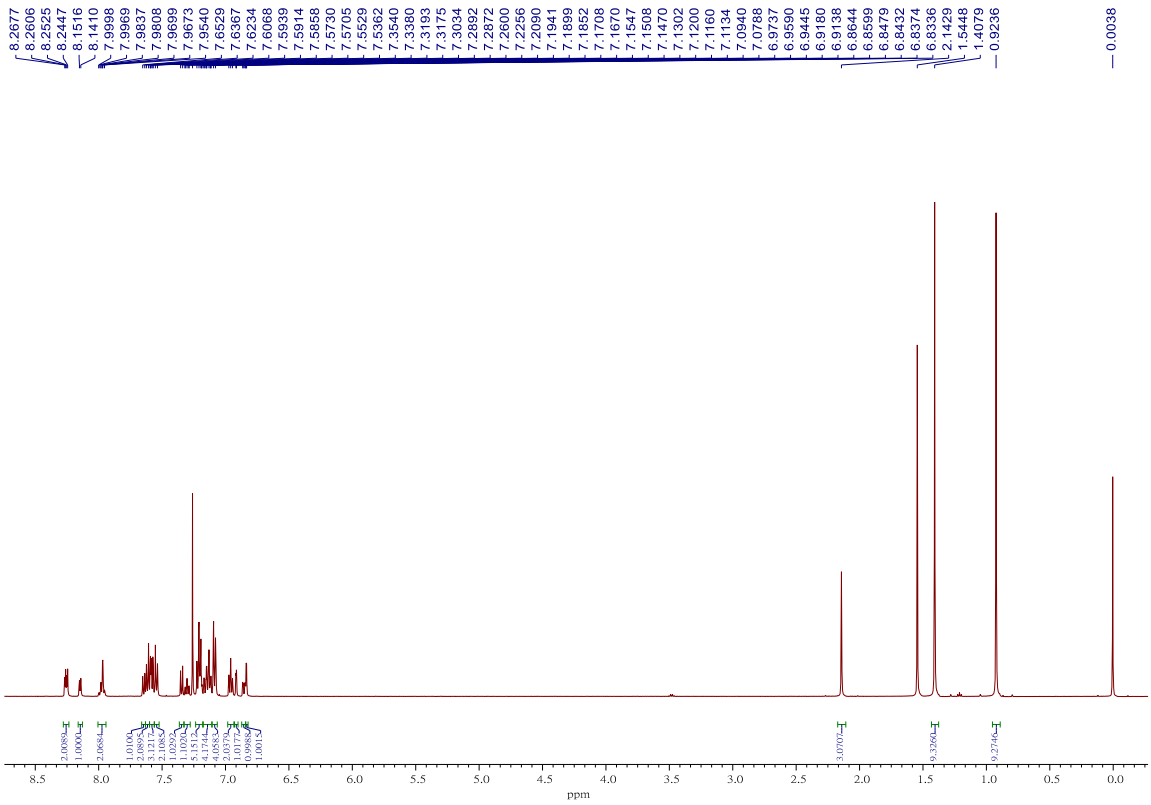

References

1. Connelly, N. G.; Geiger, W. E., Chemical Redox Agents for Organometallic Chemistry. *Chem. Rev.* **1996**, *96*, 877.
2. Yokoyama, D., Molecular Orientation in Small-Molecule Organic Light-Emitting Diodes. *J. Mater. Chem.* **2011**, *21*, 19187.
3. Moon, C.-K., *Molecular Orientation and Emission Characteristics of Ir Complexes and Exciplex in Organic Thin Films.* Springer: 2019.
4. Marcato, T.; Shih, C.-J., Molecular Orientation Effects in Organic Light-Emitting Diodes. *Helv. Chim. Acta* **2019**, *102*, e1900048.
5. Cai, X.; Li, X.; Xie, G.; He, Z.; Gao, K.; Liu, K.; Chen, D.; Cao, Y.; Su, S.-J., "Rate-Limited Effect" of Reverse Intersystem Crossing Process: the Key for Tuning Thermally Activated Delayed Fluorescence Lifetime and Efficiency Roll-Off of Organic Light Emitting Diodes. *Chem. Sci.* **2016**, *7*, 4264.
6. Xie, G.; Li, X.; Chen, D.; Wang, Z.; Cai, X.; Chen, D.; Li, Y.; Liu, K.; Cao, Y.; Su, S.-J., Evaporation- and Solution-Process-Feasible Highly Efficient Thianthrene-9,9',10,10'-Tetraoxide-Based Thermally Activated Delayed Fluorescence Emitters with Reduced Efficiency Roll-Off. *Adv. Mater.* **2016**, *28*, 181.
7. Zhang, J.; Duan, C.; Han, C.; Yang, H.; Wei, Y.; Xu, H., Balanced Dual Emissions from Tridentate Phosphine-Coordinate Copper(I) Complexes toward Highly Efficient Yellow OLEDs. *Adv. Mater.* **2016**, *28*, 5975.
8. Crosby, G. A.; Demas, J. N., Measurement of Photoluminescence Quantum Yields. Review. *J. Phys. Chem.* **1971**, *75*, 991.
9. Ellis, G. P.; Romney-Alexander, T. M., Cyanation of Aromatic Halides. *Chem. Rev.* **1987**, *87*, 779.
10. Berger, O.; Petit, C.; Deal, E. L.; Montchamp, J.-L., Phosphorus-Carbon Bond Formation: Palladium-Catalyzed Cross-Coupling of H-Phosphinates and Other P(O)H-Containing Compounds. *Adv. Synth. Catal.* **2013**, *355*, 1361.
11. Kochapradist, P.; Prachumrak, N.; Tarsang, R.; Keawin, T.; Jungsuttiwong, S.; Sudyoadsuk, T.; Promarak, V., Multi-Triphenylamine-Substituted Carbazoles: Synthesis, Characterization, Properties, and Applications as Hole-Transporting Materials. *Tetrahedron Lett.* **2013**, *54*, 3683.
12. Li, L.-K.; Tang, M.-C.; Lai, S.-L.; Ng, M.; Kwok, W.-K.; Chan, M.-Y.; Yam, V. W.-W., Strategies Towards Rational Design of Gold(III) Complexes for High-Performance

Organic Light-Emitting Devices. *Nat. Photonics* **2019**, *13*, 185.

13. Perdew, J. P.; Burke, K.; Ernzerhof, M., Generalized Gradient Approximation Made Simple. *Phys. Rev. Lett.* **1996**, *77*, 3865.
14. Perdew, J. P.; Burke, K.; Ernzerhof, M., Generalized Gradient Approximation Made Simple *Phys. Rev. Lett.* **1997**, *78*, 1396.
15. Adamo, C.; Barone, V., Toward Reliable Density Functional Methods without Adjustable Parameters: The PBE0 Model. *J. Chem. Phys.* **1999**, *110*, 6158.
16. Hehre, W. J.; Ditchfield, R.; Pople, J. A., Self—Consistent Molecular Orbital Methods. XII. Further Extensions of Gaussian—Type Basis Sets for Use in Molecular Orbital Studies of Organic Molecules. *J. Chem. Phys.* **1972**, *56*, 2257.
17. Hariharan, P. C.; Pople, J. A., The Influence of Polarization Functions on Molecular Orbital Hydrogenation Energies. *Theor. Chim. Acta.* **1973**, *28*, 213.
18. Francl, M. M.; Pietro, W. J.; Hehre, W. J.; Binkley, J. S.; Gordon, M. S.; DeFrees, D. J.; Pople, J. A., Self-Consistent Molecular Orbital Methods. XXIII. A Polarization-Type Basis Set for Second-Row Elements. *J. Chem. Phys.* **1982**, *77*, 3654.
19. Bauernschmitt, R.; Ahlrichs, R., Treatment of Electronic Excitations within the Adiabatic Approximation of Time Dependent Density Functional Theory. *Chem. Phys. Lett.* **1996**, *256*, 454.
20. Casida, M. E.; Jamorski, C.; Casida, K. C.; Salahub, D. R., Molecular Excitation Energies to High-Lying Bound States from Time-Dependent Density-Functional Response Theory: Characterization and Correction of the Time-Dependent Local Density Approximation Ionization Threshold. *J. Chem. Phys.* **1998**, *108*, 4439.
21. Stratmann, R. E.; Scuseria, G. E.; Frisch, M. J., An Efficient Implementation of Time-Dependent Density-Functional Theory for the Calculation of Excitation Energies of Large Molecules. *J. Chem. Phys.* **1998**, *109*, 8218.
22. Barone, V.; Cossi, M., Quantum Calculation of Molecular Energies and Energy Gradients in Solution by a Conductor Solvent Model. *J. Phys. Chem. A* **1998**, *102*, 1995.
23. Cossi, M.; Rega, N.; Scalmani, G.; Barone, V., Energies, Structures, and Electronic Properties of Molecules in Solution with the C-PCM Solvation Model. *J. Comput. Chem.* **2003**, *24*, 669.
24. Andrae, D.; Häußermann, U.; Dolg, M.; Stoll, H.; Preuß, H., Energy-Adjusted *Ab*

Initio Pseudopotentials for the Second and Third Row Transition Elements. *Theor. Chim. Acta.* **1990**, *77*, 123.

25. Ehlers, A. W.; Böhme, M.; Dapprich, S.; Gobbi, A.; Höllwarth, A.; Jonas, V.; Köhler, K. F.; Stegmann, R.; Veldkamp, A.; Frenking, G., A Set of f-Polarization Functions for Pseudo-Potential Basis Sets of the Transition Metals Sc-Cu, Y-Ag and La-Au. *Chem. Phys. Lett.* **1993**, *208*, 111.

26. Frisch, M. J.; Trucks, G. W.; Schlegel, H. B.; Scuseria, G. E.; Robb, M. A.; Cheeseman, J. R.; Scalmani, G.; Barone, V.; Mennucci, B.; Petersson, G. A.; Nakatsuji, H.; Caricato, M.; Li, X.; Hratchian, H. P.; Izmaylov, A. F.; Bloino, J.; Zheng, G.; Sonnenberg, J. L.; Hada, M.; Ehara, M.; Toyota, K.; Fukuda, R.; Hasegawa, J.; Ishida, M.; Nakajima, T.; Honda, Y.; Kitao, O.; Nakai, H.; Vreven, T.; Montgomery, J., J. A.; Peralta, J. E.; Ogliaro, F.; Bearpark, M.; Heyd, J. J.; Brothers, E.; Kudin, K. N.; Staroverov, V. N.; Keith, T.; Kobayashi, R.; Normand, J.; Raghavachari, K.; Rendell, A.; Burant, J. C.; Iyengar, S. S.; Tomasi, J.; Cossi, M.; Rega, N.; Millam, J. M.; Klene, M.; Knox, J. E.; Cross, J. B.; Bakken, V.; Adamo, C.; Jaramillo, J.; Gomperts, R.; Stratmann, R. E.; Yazyev, O.; Austin, A. J.; Cammi, R.; Pomelli, C.; Ochterski, J. W.; Martin, R. L.; Morokuma, K.; Zakrzewski, V. G.; Voth, G. A.; Salvador, P.; Dannenberg, J. J.; Dapprich, S.; Daniels, A. D.; Farkas, O.; Foresman, J. B.; Ortiz, J. V.; Cioslowski, J.; Fox, D. J., Gaussian 09 (Revision D.01). Gaussian, Inc.: Wallingford CT, 2013.